Chapter 1

Photoswitchable Systems for Dynamic Transfer of Chirality

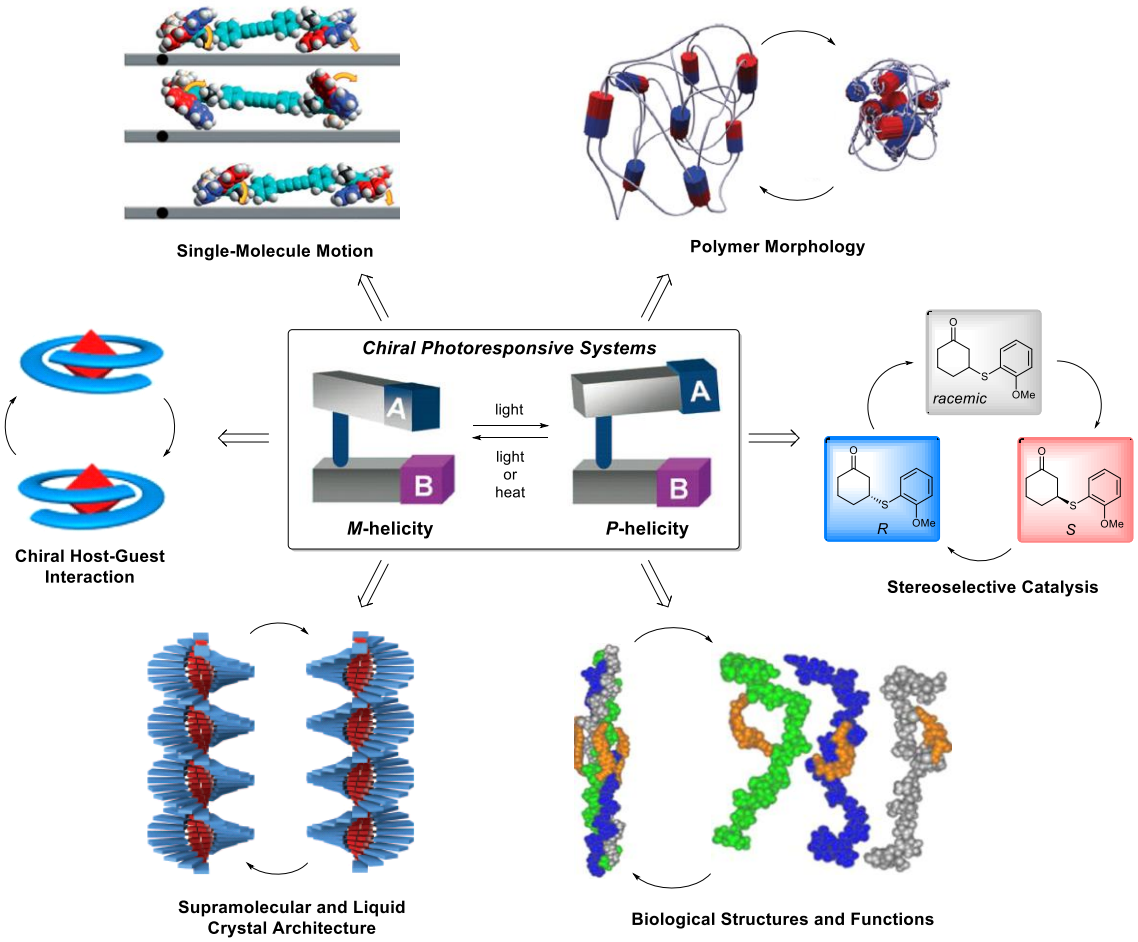

In this chapter, the concept of photo-controlled dynamic transfer of chirality is presented. After a general introduction of various versatile classes of photochromic molecules, illustrative examples using light-triggered molecular switches and motors to illustrate the concepts of dynamic transfer of chirality are discussed. Various approaches towards the chemistry of smart materials are presented, including the most relevant applications of chiral photoresponsive systems to molecular motion, liquid crystals, polymers, catalysis, host-guest complexes, and biological structures.

1.1 Chirality

Since the pioneering work of Pasteur,[1] Le Bel and van't Hoff,[2] stereochemistry[3,4] has evolved to a multifaceted and interdisciplinary field that continues to grow at an exponential rate. Today, we know that chirality can indeed be encountered at all levels in nature – in the form of elementary particle known as the helical neutrino, inherently chiral proteins, carbohydrates and DNA, or helical bacteria, plants and sea shells, up to the shapes of spiral galaxies.[5–7] Pasteur realized that chiral objects exist as a pair of enantiomorphous mirror images that are non-superimposable and related to each other like a left-handed and right-handed gloves.[1] At the molecular level, enantiomeric species can exhibit striking differences in chemical and physical properties when interacting with a chiral environment.[5] Many biologically active compounds, ranging from pharmaceuticals, agrochemicals, flavor, fragrances, and nutrients are chiral.[8] The social and economic relevance acquired by our ability of controlling chirality can be hardly overestimated. The increasing demand for enantiopure chemicals has been accompanied by significant progress in asymmetric synthesis and catalysis, and by the development of analytical techniques for the determination of the stereochemical purity of chiral compounds. Stereoselective analysis usually entails chiroptical measurements, NMR spectroscopic and mass spectrometric methods, electrophoresis, chiral chromatography or UV and fluorescence sensing assays. Furthermore, in depth stereoselective analysis can provide invaluable information about the stability of chiral compounds.

1.2 Organic photoswitchable molecules

The desire to control and manipulate molecular structures by an external stimulus such as light has been inspired by the photoinduced movements and morphogenesis frequently encountered in nature. A prominent example is the visual excitation in retina based on light-induced *cis-trans* isomerization of 11-*cis*-retinal to all-*trans*-retinal.[9] This process essentially converts a single photon into molecular motion through conformational changes, triggering an enzymatic cascade and subsequently a nerve pulse. Retinal isomerase then regenerates *cis*-retinal which basically serves as photoresponsive biomolecular switch.

During the last decades, chemists have developed various classes of artificial responsive systems and switches. Important properties of a molecular switch are bistability and fast, effective and reproducible responsiveness to a photochemical, thermal, electrochemical or chemical stimulus. A bistable system consists of two stable states that undergo reversible interconversion controlled by an external signal. Other criteria for the usefulness of a switch are detectability and non-destructive read-out, stability to photochemical and thermal degradation, and stability to interconversion and concomitant loss of information over a wide range of temperatures.

The photochemistry of fulgides, azobenzenes, spiropyrans, diarylethenes and sterically overcrowded stilbenes that undergo photochemically controlled *cis-trans* isomerization, cyclization, electron transfer, and tautomerization has been exploited for the same purpose. A typical photochemical process starts with the absorption of a photon, causing the excitation of an electron from an occupied orbital, often the highest in energy (*HOMO*), to an unoccupied orbital, often the one lowest in energy (*LUMO*). From this excited state the system can relax back to its ground state via radiative processes (*fluorescence* or *phosphorescence*) or thermal processes (*internal conversion*). Photochromism is an alternative photochemical reactivity that has interested chemists for decades.[10,11] It is defined as the reversible photochemically driven transformation between two isomers displaying different UV-vis absorption spectra. Photoreversible switching relies on selective interconversion of distinct isomers that absorb at different wavelengths. Chiral photochromic compounds are susceptible to selective diastereomerization and enantiomerization induced by irradiation at different wavelengths or circularly polarized light, respectively. Attractive features of chiroptical switches commonly include facile non-destructive read-out and detectability by ORD or CD spectroscopy at wavelengths remote from absorption maxima. Compounds exhibiting this behavior attracted much interest as they can be used as molecular switches[12,13] and applied in more complex systems, such as in organic electronic devices[14] or optical data storage.[15,16] The most relevant classes of organic photochromic molecules are depicted in Scheme 1.1.

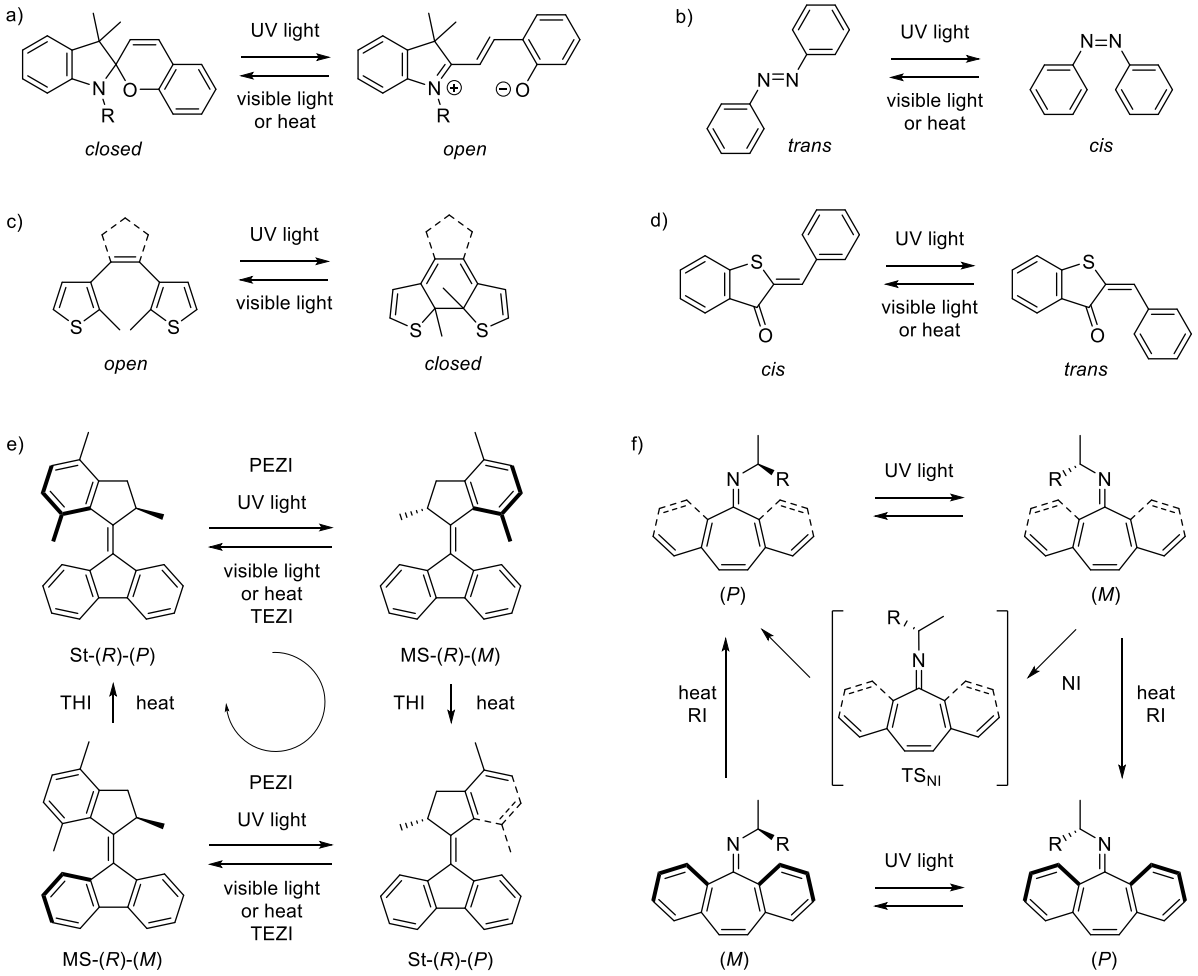

Scheme 1.1. Photochemical and thermal reactivity of main classes of photochromic molecules: a) spiropyrans; b) azobenzenes; c) diarylethenes; d) hemithioindigos; e) overcrowded alkenes (here an example of second generation molecular motor is displayed; f) diaryl-*N*-alkyl imines.

Spiropyrans consist of two fused heterocyclic rings, one of which is a pyran derivative (Scheme 1.1a).[17,18] Irradiation of UV-light induces the conversion of a spiropyran into a zwitterionic merocyanine isomer, which absorbs strongly in the visible region. The reverse isomerization process towards the starting pyran form can be achieved by irradiation with visible light. Alternatively, the conversion of the merocyanine isomer can also proceed thermally, although thermally stable merocyanine isomers have been described.[19]
Azobenzenes consist of two phenyls attached to a central azo moiety (Scheme 1.1b).[20,21] The typically more energetically favored *trans*-isomer can be converted to the more sterically hindered *cis*-isomer upon irradiation with UV light. The reverse isomerization process can be induced either by irradiation with visible light or thermally. The UV-vis absorption spectra as well as the thermal stability of azobenzenes is strongly dependent on the electronic properties of the substituents and the substitution pattern on the phenyl rings.
Similar to azobenzenes, diarylethenes consist of two aromatic groups connected to a central double bond (Scheme 1.1c).[22,23] However, the structure of a cyclic olefin cannot accommodate a *cis-trans* isomerization upon photochemical excitation. Instead, the compounds undergo a conrotatory six-electron electrocyclization yielding a ring-closed isomer. As opposed to spiropyrans and azobenzenes, the photo-generated closed isomer is thermally stable and requires irradiation with visible light to obtain the initial open-ring isomer. The most popular design for diarylethenes features two thiophene rings and is referred to as dithienylethenes.

Hemithioindigos switches consist of a hemithioindigo moiety and a hemistilbene moiety joined at the central olefin (Scheme 1.1d).[24–26] The *Z*-isomer, typically lower in energy, can be converted to the corresponding *E*-isomer, higher in energy, by irradiation with UV-light. The isomerization takes place with concomitant bathochromic shift of the UV-vis absorption band, which allows reversing the isomerization bias by irradiation at longer wavelength. In some systems the reverse *E-Z* isomerization can also take place thermally.

Overcrowded alkenes represent a unique class of chiroptical photochromic compounds, displaying rotation around a sterically hindered central olefinic bond.[13] They are able of repetitive photoinduced *E-Z* isomerization as their molecular structure, i.e. steric properties and substitution pattern, effectively suppress the competing electrocyclization process that affects simpler stilbene systems.[27] With the introduction of stereogenic center(s), this type of chiroptical switches is capable of making a complete rotation around the central olefin (Scheme 1.1e).[28] The stereogenic causes the product of the photochemical *E-Z* isomerization (PEZI) to lie higher in energy (*metastable* or *unstable* form) and adopt an opposite helicity. This is due to the steric hindrance which impedes the two halves to complete a full 180° rotation relative to each other. Forward and backward isomerization can generally be obtained by irradiation with UV-light of different wavelength or UV-light and visible light, respectively, depending on the absorption spectra of the distinct stable and metastable isomers. Depending on the structural design of the switch, thermally induced relaxation of the metastable state can proceed via reverse thermal *E-Z* isomerization (TEZI), yielding the starting isomer with net 0° rotation, or via thermal helix inversion (THI), yielding a second stable form with net 180° rotation and same helicity of the starting stable isomer upon structural deformation and slipping of one half other the other. The energy barrier for THI is mainly influenced by the flexibility of the overcrowded alkene structure.[29] Repeating the *E-Z* isomerization and subsequent helix inversion cause the system to return to its original state at which point one full rotation has been made. Systems displaying this behavior are referred to as molecular motors. Depending on the number of stereogenic centers and symmetric of the rotating units, molecular motors are divided into *first* (two),[30] *second* (one)[31] and *third* generation (zero).[32] The unique photochromic and thermochromic properties of overcrowded alkenes originate from significant ground state distortion, molecular twisting and bistability of stereoisomeric states. The equilibrium of *cis*- and *trans*-isomers at the photostationary state is determined by the ratio of the molar absorption coefficients of the two diastereoisomers at the wavelengths used and the ratio of the quantum yields of each diastereoisomerization reaction. Since the interconverting isomers of overcrowded alkenes exist as mixtures obeying Boltzmann distribution and reversible reaction kinetics, molecular motors do not in fact rotate in an exclusively monodirectional sense. However, the discrete and synergic photochemical and thermal isomerization reactions of the diastereomeric mixtures result in an overall unidirectional rotary motion observed from the stator.

More recently, an analogous type of rotary molecular motor based on imine *syn–anti* isomerization has been developed .[33] Similar to alkenes, imines may undergo both photochemical and thermal isomerization. Directionality can be forced on these processes by introducing a stereogenic center on the *N*-substituent of the imine functionality, yielding unidirectional molecular motors (Scheme 1.1d).[34,35] The design is based on diaryl-*N*-alkyl imines, which are stable towards thermal *E–Z* isomerization at ambient temperatures. Irradiation of a diastereomeric mixture leads to photoisomerization at the C=N bond and a shift of the equilibrium towards the (*M*)-isomer. The original diastereomeric ratio was restored after a thermal relaxation. This thermal reaction was proposed to proceed through two different mechanisms. Inversion at the nitrogen (NI) moves the substituent back to its original position. Alternatively, the system can release the steric strain via ring inversion (RI) of the less energetically favored (*M*)-form, regenerating the more stable (*P*)-form through an effective 180° rotation. Via the ring inversion mechanism, the system described is able to able to undergo a complete unidirectional 360° rotation in four steps similarly to overcrowded alkenes-based motors.

1.3 Dynamic stereochemistry and molecular motors

1.3.1 Chirality sets the way

Stereochemistry embraces a broad variety of closely intertwined static and dynamic aspects that are all related to the three-dimensional structure of molecules. While static stereochemistry deals with the spatial arrangement of atoms in molecules and the corresponding chemical and physical properties, dynamic stereochemistry emphasizes structural change and comprises asymmetric reactions as well as interconversion of configurational and conformational isomers.[36] Dynamic stereochemistry plays a fundamental role across the chemical sciences, ranging from asymmetric synthesis to drug discovery and nanomaterials. It is also a distinctive feature encountered in biological systems, crucial for precise regulation of numerous chirality-dependent metabolic processes (e.g. DNA-helix, protein α-helix, conformation of sugars, bacterial flagella, etc.).[6] The unique stereodynamics of chiral compounds have paved the way to artificial machines and other molecular devices that lie at the interface of chemistry, engineering, physics, and molecular biology.[37] The design of molecular gears, rotors, switches, bevel gears. scissors, brakes, shuttles, turnstiles, sensors and even motors showing unidirectional motion has certainly been inspired by the coordinated movement in biological systems such as muscle fibers, flagella and cilia or in macroscopic conventional machines.[38–41] Feringa and co-workers developed light-driven molecular motors derived from sterically overcrowded chiral alkenes exhibiting thermal bistability and non-destructive read-out.[42] Among the various examples of photoresponsive molecular systems, molecular motors certainly stand out for their unique motion mechanism governed by the interaction of fixed and dynamic chirality.[43,44] The subtle interplay between the stereogenic center and the inherently helical conformation of this type of light- and heat-responsive selectors provides control of the rotation and helicity about the central carbon-carbon double bond. Both chirality and conformational flexibility are essential for unidirectional motion of the rotor around the stator. Their dynamic chirality based on *cis-trans* photoisomerization and thermally induce helix inversion provides a versatile and powerful tool for induction of chiral information in a reversible fashion.[45] In the next sections, popular examples of applications of molecular switches and motors for control of dynamic transfer of chirality will be discussed. The dynamic chirality of such systems is exploited to selectively induce a reversible and reproducible non-symmetrical response, which is, for instance, directional motion, a specific chiral supramolecular morphology, asymmetric catalytic outcome, chiral recognition or a biological activity. Further details on this topic are summarized in comprehensive subject-related reviews.[37,41,46–49]

1.3.2 Control of single-molecule motion

Nature provides many wonderful examples of molecular machines including motor proteins that perform a variety of tasks like chromosome segregation,[50] cellular trafficking,[51] and locomotion.[52] By contrast our current technology, with the exception of liquid crystals, is still far from utilizing productively the nanoscale motion of molecules.[39] Indeed, the ability to control molecular motion by means of non-invasive stimuli represented a prominent challenge since the birth of artificial chiroptical switches.[13] Often inspired by the mechanical elements of conventional machine engineering, devices like molecular gears, rotors, shuttles, etc. have been developed with the future prospect of combining each of their specific function to eventually build complex and efficient supramolecular machines.[53] Molecular motors constitute themselves a clear example of internal dynamic transfer of chirality, for which the fixed point chirality of the stereogenic center(s) dictates the sense of unidirectional motion around the olefinic bond through multiple states with selectable helicity.[54] Their rotative isomerization mechanism makes them excellent candidates for achieving transport at nanoscale by directional motion on surfaces. Their rotation mechanism relative to an adsorbed surface can be considered a dynamic transfer of chirality, as a preferential direction of translational motion is stereospecifically achieved upon isomerization of the embedded photoresponsive core along a defined sense of rotation. Nanovehicles are molecules resembling a regular car, containing wheels, axes and a chassis.[55] The group of Tour developed various classes of nanoscale vehicles, ranging from a car,[56] to a dragster,[57] and a train[58] that could be deposited and pushed using an STM tip. The group

realized the first nanocar propelled by a photoswitchable overcrowded alkene incorporated in the central chassis and featuring four carborane wheels **1** (Figure 1.1a).[59] The proposed motion mechanism entailed moving the car over the surface with a skipping motion. Despite the rotational properties of the motor embedded in the nanocar were found to be very similar to the parent motor in solution, the strong interaction between the nanocar and the adsorbed copper surface impede any lateral motion induced by light or STM tip pushing. Movement of the motorized nanocar across the surface was eventually induced by pulses from the STM tip. Subsequently, the group of Tour demonstrated light-induced movement of a motorized 'nanoroadster' **2** on the surface (Figure 1.1b).[60] The roadster consists of a fast unidirectional overcrowded alkene based second generation molecular motor attached to an axle with two adamantane wheels. At temperatures above 150 K, the roadsters start to diffuse across the Cu(111) surface. Irradiation causes the molecular motor to skip across the surface and increase the speed of diffusion. However, the direction of movement displayed by these roadsters is random.

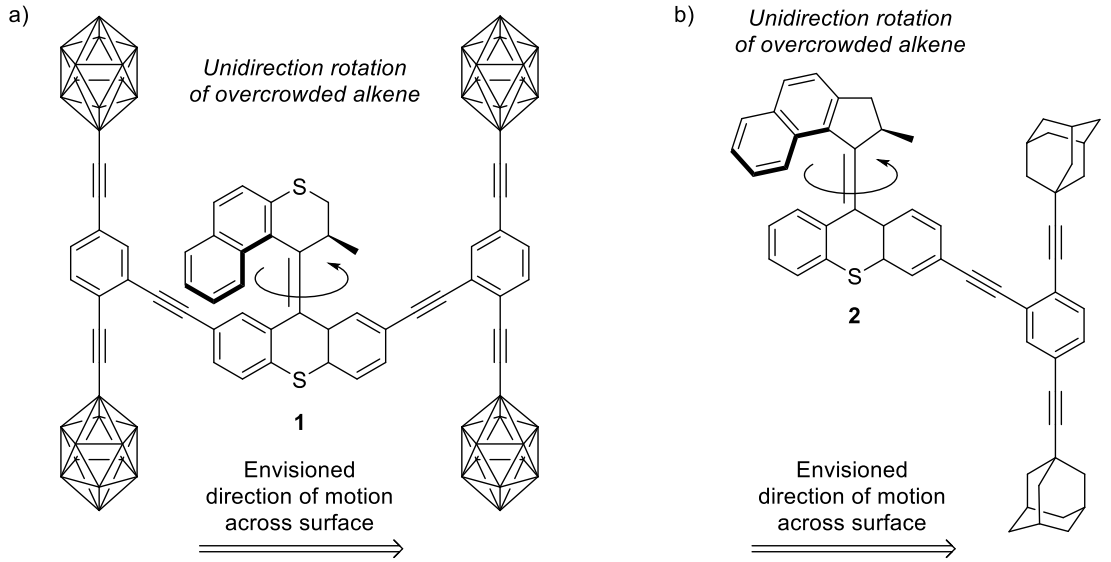

Figure 1.1. Schematic representation of structure and envisioned dynamics of motion across the metal surface of nanocar (a) and nanoroadster (b) developed by Tour and co-workers.

Feringa, Ernst and co-workers reported a nanocar **3** that is capable of unidirectional motion over a copper surface powered by electrons from the tip of a scanning tunneling microscope (STM) (Figure 1.2).[61] Feringa and co-workers carefully constructed the nanocar with four switchable wheels that had different chirality on opposite sides of the molecule. This provided the necessary asymmetry and yielded motion only in the forward direction, as in all the four wheels were sequentially rotating in accordance to provide the same translational motion. Notably, only the meso-(*R*,*S*-*R*,*S*)-isomer is capable of directional movement, provided that the nanocar underwent the correct asymmetric 'landing mode'. Ernst's group used voltage-dependent experiments in which tunneling electrons of different energies were used to excite the molecule, while its motion was measured by STM imaging before and after excitation. These studies revealed that the motors inched forward through a sequence of lower energy (ca. 20 kJ mol^{-1}) helix inversions driven by vibrational excitation and higher energy (ca. 50 kJ mol^{-1}) C=C isomerizations induced through an electronically excited state of the motor. Only molecules with the correct chirality of wheels exhibited directional (almost completely straight) motion whereas molecules in which the wheels on opposite sides of the chassis turned in opposite directions resulting in spinning and random motion [(*R*,*R*-*R*,*R*)-isomer]. Although the temperatures at which the nanocar operates make this type of system far from being useful in practical devices and the system was operated by electronic stimuli rather than by light-irradiation, it is one of a small number of studies that offer insight into how energy is transferred into motion at the single-molecule level by operating stimuli-responsive chiroptical switches.

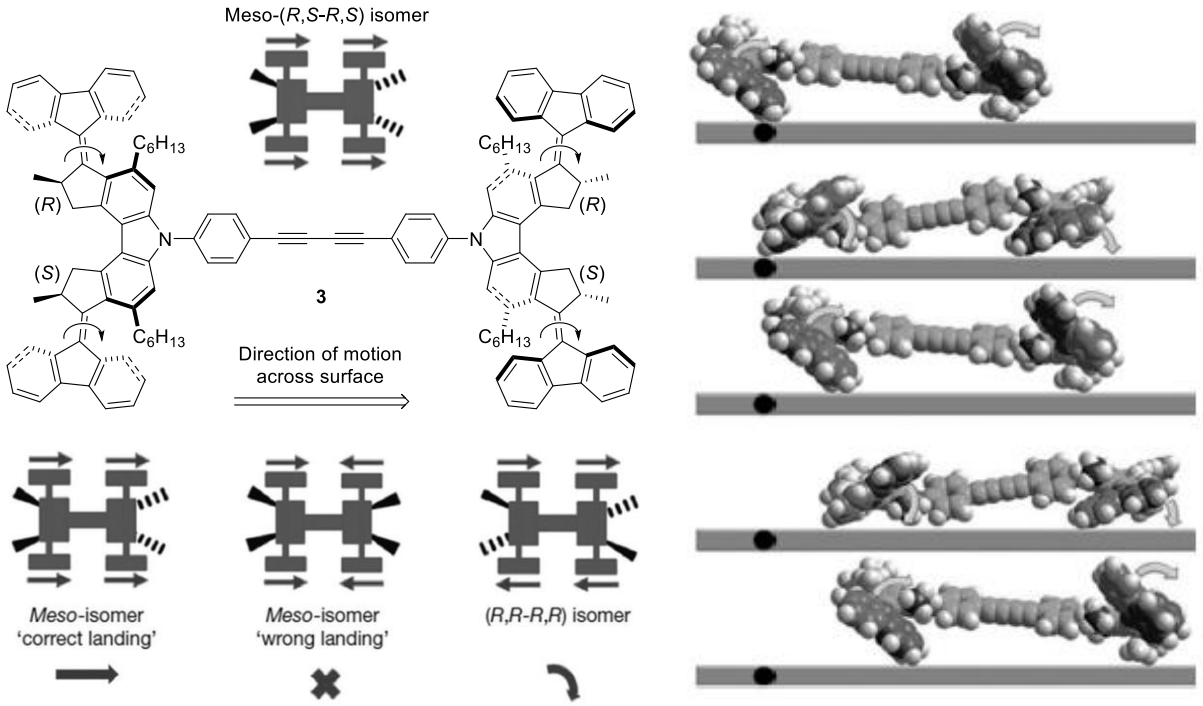

Figure 1.2. Schematic representation of the nanocar's structure and dynamics of its motion across the metal surface, developed by Feringa and Ernst and co-workers. Reproduced with permission from Ref. 61.

Additional investigation on the possibilities of controlling molecular motion on surfaces with third generation molecular motors can be found in the work of Štacko[62] and Heideman.[63] The design of third generation molecular motors, each composed of two rotating 'wheels', allows simplifying the nanovehicle synthesis and reducing its molecular weight. Upon selection of the appropriate size of olefin-bridged cycloalkenes and substituents in the fjord region, applications at room temperatures and under light-irradiation have been explored. The reader is strongly invited to consult their theses and manuscripts for further details.

Notably, the synthesis of the four-wheeled motorized nanocar required 13 synthetic steps and chiral HPLC separation, with an overall yield of 1.3%. No practical application of such systems can be considered readily feasible or interesting for practical applications. Therefore, for larger scale applications, chemists need to rely on other methods, such as cooperativity and synchronization between clusters of dynamic molecules and amplification of motion. Such properties are more likely to be featured by systems based on supramolecular assemblies, polymer chemistry or surface functionalization. Functionalization of surfaces with responsive units[64–66] represents an alternative approach, providing smart control of surface related properties; for instance wettability or adhesion based on dynamic interaction with objects incapable of autonomous motion. However, this alternative would require a highly ordered placement of the interacting layer, possibly harnessing the amplification effects provided via self-assembling of supramolecular systems and neighboring chiral induction by responsive dopants.

1.3.3 Liquid crystal and supramolecular structure morphology

Transmission of chiral information from single-molecule to macromolecular levels[67] is a powerful mechanism adopted in nature for the controlled self-assembly of chiral subunits into complex superstructures. This results in well-defined architectures capable of regulating highly specific biological functions due to their unique three-dimensional molecular shapes (e.g. DNA-helix, enzymes, hormone receptors, ion-channels, etc.).[6] Helical domain(s) in macromolecules such as starch, protein, and DNA may thus be generated,[68,69] while H-bonding, electrostatic, π-π, and van der Waals (vdW) interactions are the major molecular forces involved in triggering these self-assembly processes. As inspired by Nature, synthetic systems offer a diverse array of opportunities to control the properties of materials in a dynamic,

modular and even reversible manner. By taking advantage of these molecular forces, one can also trigger the self-assembly of custom-designed small molecules into large supramolecular aggregates, liquid crystal domains or gel networks.[70] The ordered arrangement in such complex systems made by physical interplay can be perturbed by forces including heat, light, chemical additives, and mechanical action.[71]
A dominant theme within the research on two-dimensional chirality is the sergeant–soldiers principle,[72] wherein a small fraction of chiral molecules (sergeants) is used to direct the handedness of achiral molecules (soldiers) to generate a homo-chiral structure.[73] The general principles of supramolecular chemistry have proven particularly useful for understanding the different aspects of light-responsive chiral induction phenomena.[74] Conversely, the handedness of a supramolecular aggregate can also be used as a probe to comprehend the fundamentals of amplification of chirality in supramolecular aggregates.[75]
Feringa, Eelkema and co-workers described the unidirectional rotation of a macroscopic glass rod deposited on a light-responsive liquid crystal film (Figure 1.3).[76] A cholesteric liquid crystal film was doped with an enantiopure second generation molecular motor **4** (1 wt%). Continuous irradiation of the fast-rotating molecular motor around the central alkene bond causes a repeated change in its helicity. When the motor is used as a dopant, the liquid crystal adopts the same helicity through a 'sergeants-and-soldiers' principle.[72] Upon irradiation of the sample, rearrangement of the liquid crystal occurring in a clockwise fashion is observed. A microscopic glass rod, deposited on top of the liquid crystal layer was used to visualize the moving liquid crystal pattern. Irradiation with 365 nm light caused the rod to rotate in a clockwise manner. The movement was observed over 10 min of continuous stimulus, after which period the response gradually halted. The motion resumed in an anti-clockwise direction upon removal of the irradiation source. A control experiment using the opposite enantiomer induced rotation in the opposite direction. After an in depth investigation, it was concluded that the rotation of the glass rod is a direct result of the switching helicity of the dopant, rather than the unidirectionality of the rotation of the motor.[77]

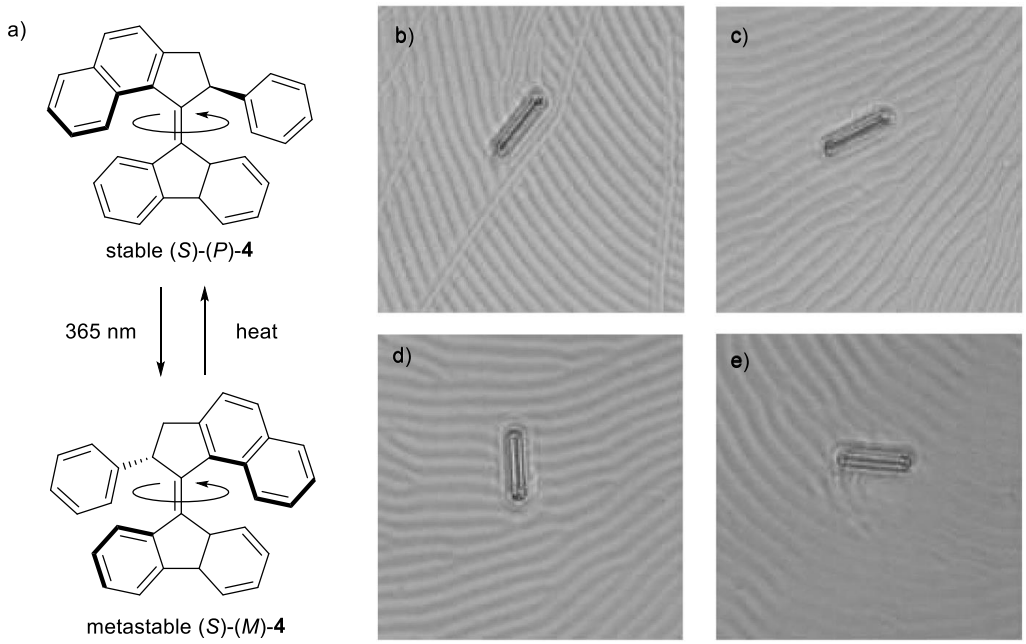

Figure 1.3. Unidirectional rotation of a macroscopic glass rod driven by pattern reorganization in a liquid crystal (only two stages of the rotary cycle are shown for simplicity) described by Feringa and co-workers. a) Structure of the molecular motor dopant **4**. Microscope images depicting initial orientation of glass rod on liquid crystal surface (b) and subsequent orientations after continuous irradiation: 28°, 15 s (c); 141°, 30 s (d); 226°, 45 s (e). Reproduced with permission from Ref. 76.

Chen and co-workers developed photoswitchable helicenes **5** as conformation modulable photochromes capable of transferring their reversible, complementary helicities in chiral liquid-crystalline materials upon

light-induced switching (Figure 1.4).[78] The structure of such helicenes comprises a C_2-symmetric dibenzosuberane (DBS) stator featuring two chiral centers and a biaryl-functionalized rotor joined at the central olefin. Similar to overcrowded alkene-based switches, the fixed chirality on the stereogenic centers dictates the dynamic structural helicity adopted in the two addressable states. The helicenes incorporated aromatic amide ("aramide") moieties in the top DBS unit. In addition to H-bonding and π-π interactions, extra vdW forces were introduced by appending long-chain alkyl groups at the aramides substituents to effect interchain alignment, further facilitating organogel formation. Furthermore, a phenyl ring was introduced at the C8′ position of the bottom unit template to enhance the π-π interactions and thus the helical nature of the resulting organogels. Highly diastereoselective and complementary switching selectivities could be achieved in *n*-hexane or CH_2Cl_2 upon photoirradiation of (*M*)-**5** at 270 nm [(*M*)-**5**:(*P*)-**5** = <1:>99] and (*P*)-1′ at 335 nm [(*M*)-**5**:(*P*)-**5**, 90:10] (Figure 1.4a). Notably, a pseudoracemic mixture [(*M*)-**5**:(*P*)-**5** = 50:50] was obtained upon irradiation at 308 nm. (*M*)-**5** and (*P*)-**5** remained dissolved in apolar solvents (*n*-hexane, cyclohexane, benzene, and toluene) even at relatively high concentration (0.01 M) at ambient temperature but formed gels in more polar solvents (CH_2Cl_2, $CHCl_3$, and CH_3CN) at a minimum concentration of 1×10^{-3} M. The resulting gels were stable at ambient temperature, and the gel-to-sol interconversion was reversible upon repetitive heating (≥35 °C) and cooling cycles. Notably, (*M*)-**5** and (*P*)-**5** helicenes led to the corresponding (*M*)- and (*P*)-form helical fibers. Thus, the absolute chirality of the helicene dictates the overall helical chirality of the self-assembled helical fibers, presumably through intermolecular H-bonding and π-π interactions. In a series of TEM images taken from these photoisomerization experiments, only either pure (*M*)- or (*P*)-form bundled fibril tubes were observed when the overall composition ranged from (*M*):(*P*) = >99:<1 to 70:30 and 25:75 to <1:>99, respectively (Figure 1.4b). Notably, increasing amounts of micelles or vesicles were observed for the intermediate gel and sol states.

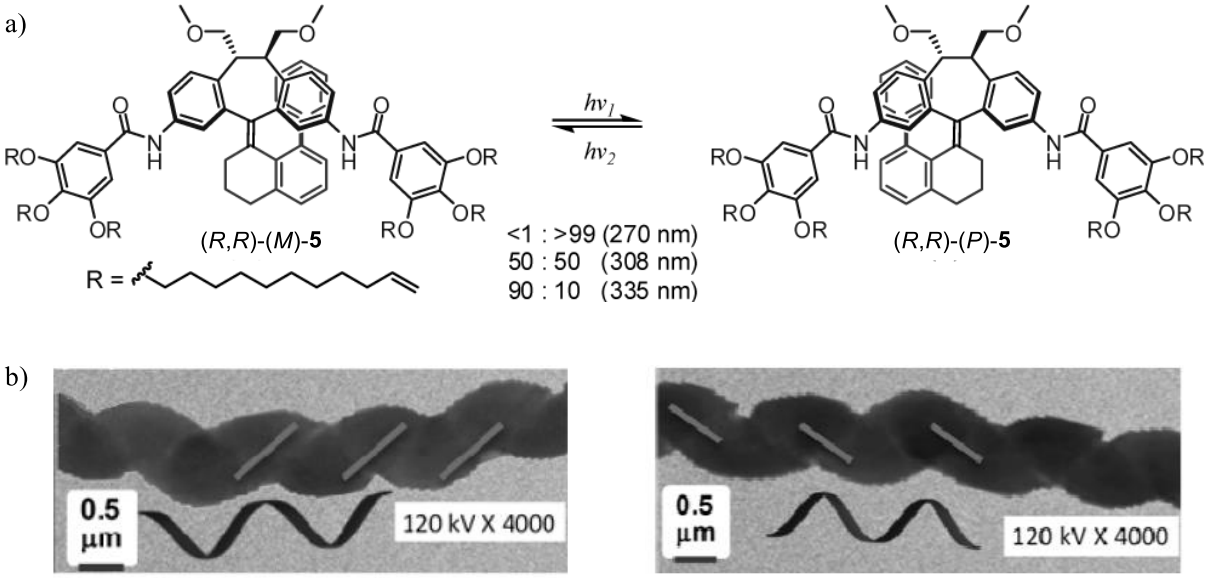

Figure 1.4. Photoisomerization profiles of C_2-symmetric dibenzosuberane-based helicenes **5** as tunable units in chiral liquid-crystalline materials developed by Chen and co-workers. b) TEM images of the bundled superstructures of xerogels from (*M*)-**5** (left) and (*P*)-**5** (right). Reproduced with permission from Ref. 78.

In order to apply photoinduced cholesteric helix inversion to the creation of new materials and devices, photoactive enantiopure dopants will have to be conveniently accessible in reasonable quantities. Consequently, researchers have investigated the possibility to use other classes of molecules as photoswitchable chiral dopants, most of them based on *cis-trans* isomerization of locally achiral photochromes incorporated in chiral structures (Figure 1.5). The groups of Feringa and Spada reported

light-induced helix inversion in cholesteric mesophases by using a BINOL-based azobenzene as a dopant. Feringa and co-workers reported that a binaphthyl-based core ensuring chiral induction, symmetrically functionalized by two azobenzene moieties, **6** yields reversible helix-inversion in a nematic host (Figure 1.5a).[79] Spada and co-workers reported a binaphthyl substituted with one azobenzene **7** (Figure 1.5b) displaying a reverses in sign of helical twisting power under UV irradiation in a nematic host.[80] Reversible helix inversion was also achieved via a combination of photochemical and thermal isomerizations of chiral azobenzenophane derivatives **8** (Figure 1.5c) dissolved in nematic hosts.[81] However, a drawback of azobenzene derivatives lies in their lack of thermal stability. The search for versatile and efficient dopants allowing helix inversion, with high helical twisting powers, remains an on-going challenge.

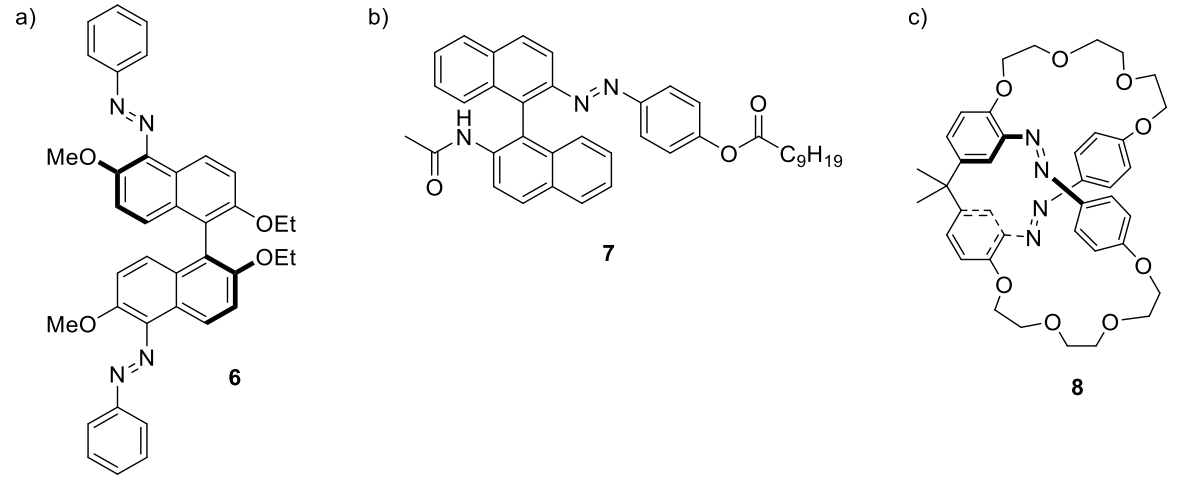

Figure 1.5. Photo-responsive dopants promoting helix inversion in cholesteric liquid crystals featuring azobenzene moieties.

1.3.4 Polymers morphology

Several synthetic polymers have been developed that exhibit a strong optical activity due to the helical conformation, with an excess of one particular handedness adopted by their backbone.[82,83] These systems have provided valuable insight into cooperative processes and the amplification of chirality in macromolecules.[84] The amplification of chirality via transfer of chiral information through non-covalent interactions to helical polymers has now been well studied, experimentally and theoretically.[85–87] For a number of these polymers (e.g. polyisocyanides or polymethacrylates bearing bulky side-groups) this helical conformation is completely locked due to strong steric interactions experienced by the side-groups of the neighboring monomeric units. However, much interest is recently devoted to macromolecules in which the helical conformation is dynamic, and rapidly inverts at ambient temperatures: the low helix inversion barriers of these polymers result in their helical conformation being thermodynamically controlled.[88,89] Moreover, due to the favorable interactions between the monomeric units in the helical conformation of these macromolecules they exist as long strands of one particular handedness, only rarely interrupted by a helix reversal along the chain. Therefore a strong preference for a particular handedness can readily be biased by a small chiral input.

In order to obtain photochemical control of the chirality of a dynamically helical polymer,[90,91] Zentel and co-workers introduced azobenzene photochromic groups containing two stereocenters in the side-chains of co-polyisocyanate **9** (Figure 1.6a).[92] The polymer was prepared with all of the azobenzene moieties adopting the *trans* configuration, and this polymer was shown to have a significant CD and ORD signal, indicating a preferred helical twist sense of the polymer. Irradiation with UV-light (365 nm) resulted in a *trans-cis* isomerization of the azobenzene groups, and resulted in a clear inversion of the CD and ORD signals (Figure 1.6b), indicating an inversion of the preferred helical twist sense of the polymer chain. The reason for this effect is not clear (the stereocenters do not change upon photoisomerization): the change in

interactions of the stereocenters at the azobenzene with the polymer backbone upon photoisomerization are proposed to cause the helical inversion.[93]

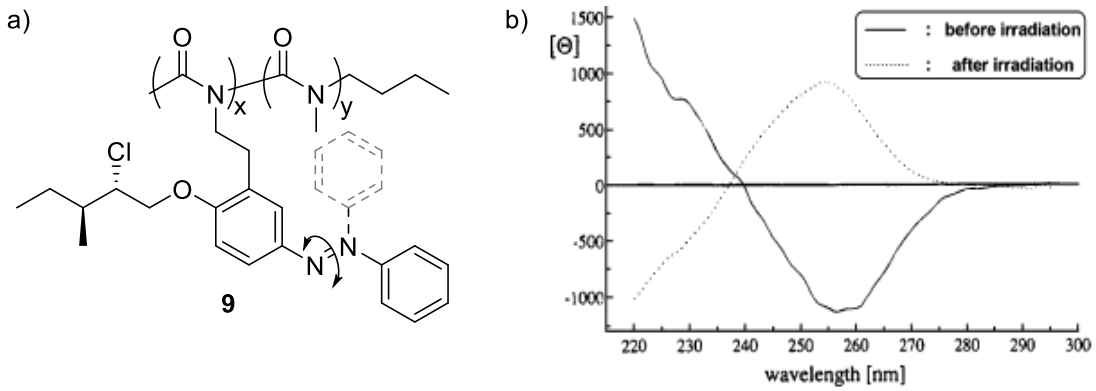

Figure 1.6. a) Co-polyisocyanate **9** containing a photochromic azobenzene group in the side chains (avg. content: 8%) developed by Zendel and co-workers. b) CD spectra of the polymer before and after the photochemically induced *trans-cis* isomerization of the azobenzene units. Reproduced with permission from Ref. 92.

In the last system, the chiral information of multiple photochromic units randomly distributed along the polymer chain is transferred to the polymer backbone. Alternatively, the presence of one chiral unit situated at the terminus of the polymer chain, introduced by the use of an optically active initiator for the polymerization, can induce a preferred helical twist sense of the polymer.[94] Reverse of polymer chain handedness can be induced upon isomerization of a chiral photo-responsive selector installed at the chain-end of the polymer. Here, the extent to which the chiral unit influences the polymer depends on the persistence length of the polymer chain: the chiral information will be transferred along the polymer backbone until a helix reversal is encountered, after which the chiral influence is lost. Therefore, the optical rotation of these helical polymers depends greatly on their chain length and temperature.
Feringa, Pijper and co-workers reported polyisocyanate **10**, in which a single chiral photochromic unit — a light-driven four step rotary molecular motor — is situated at the terminus of an intrinsically dynamically racemic helical poly(*n*-hexylisocyanate) (Scheme 1.2).[95] Due to the helical structure of the sterically overcrowded motor molecule, a chiral environment is created at the terminus of the polymer chain, which is introduced at its fluorenyl lower half. Through the four subsequent stages of the rotation process, the stereoinduction towards the macromolecule, which is generated by the cyclopentane-naphthyl upper half of the motor molecule, strongly changes (Scheme 1.2a). In this system, a single chiral photochromic switch unit attached at the terminus of a helical polymer allows the reversible induction and inversion of the preferred helical twist sense of the polymer's backbone and a three state switching cycle with racemic, *P* and *M* helicity of the polymer (Scheme 1.2b).

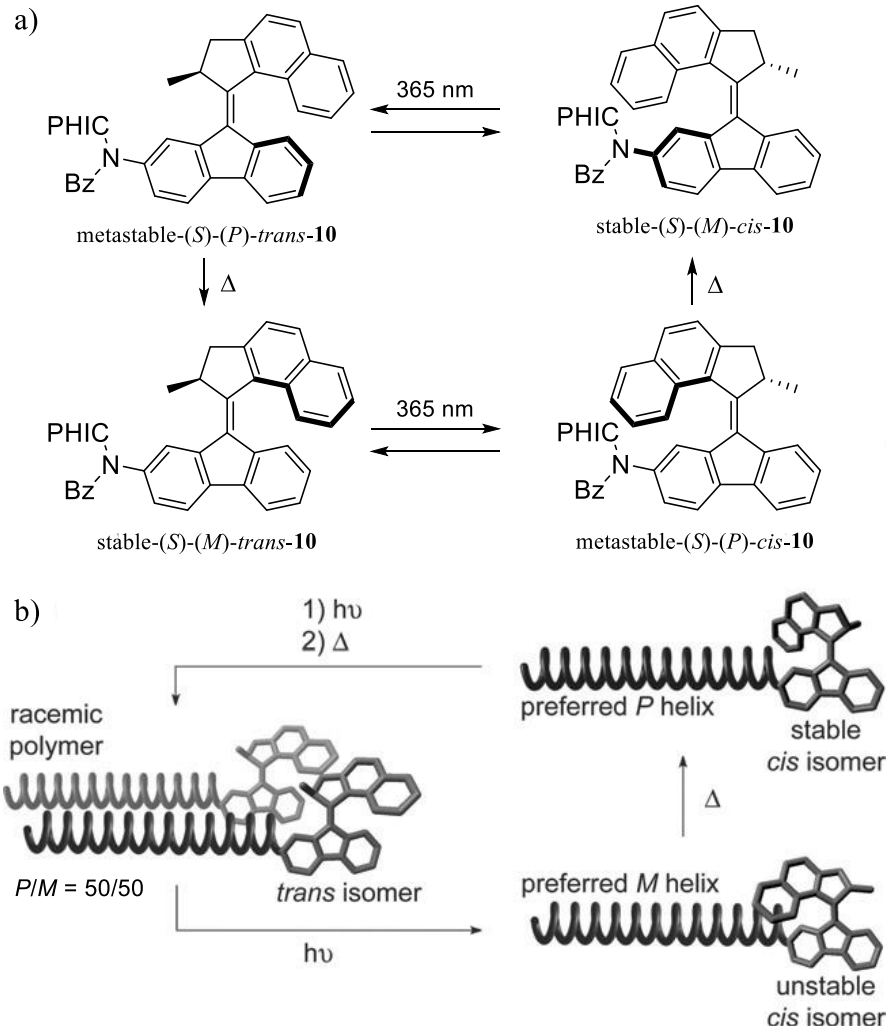

Scheme 1.2. Dynamic transmission of chirality from a light-driven rotary molecular motor to the macromolecular level of a polyisocyanate 10, as described by Feringa and co-workers. a) Unidirectional rotation cycle of chain-end motor. b) Schematic illustration of the reversible induction by chain-end motor and inversion of the helicity of a polymer backbone. Reproduced with permission from Ref. 95.

A drawback of the parent system **10** is the fact that controlling of the exact composition of the mixture of isomers of the motor molecule, and the associated chiral induction towards the polymer chain, upon irradiation at room temperature is a highly complex process. This is caused by the non-perfect photostationary states at the photochemical steps, and the fact that the thermal isomerization steps proceed relatively fast at room temperature. In order to obtain better control over the chiral induction towards the helical polymer, the photochromic unit attached at the polymer chain's terminus was redesigned into a photochemically bi-stable chiroptical switch with two thermally stable states, achieved via a slight structural modification of the molecule, and attachment of the polymer to its upper half. With this system **11** (Scheme 1.3), the magnitude and sign of the supramolecular helicity of the polymeric cholesteric LC phase can be fully controlled using two different wavelengths of light (365 nm and >480 nm).[96]

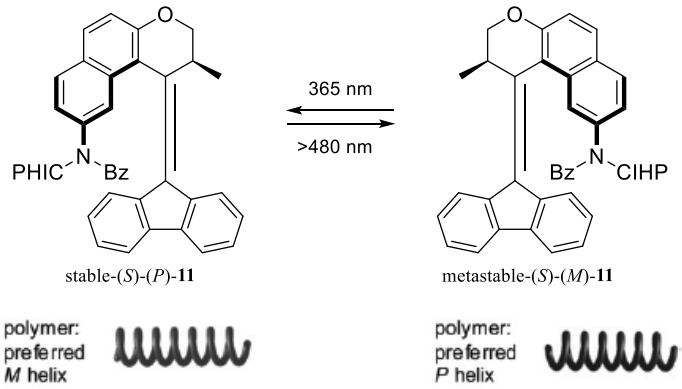

Scheme 1.3. Schematic representation of the full photocontrol of the magnitude and sign of the supramolecular helical pitch of a cholesteric LC phase generated by a polyisocyanate **11** with a single chiroptical molecular switch covalently linked to the polymer's terminus developed by Feringa and co-workers. Reproduced with permission from Ref. 96.

Recently, Feringa, van Leeuwen and co-workers investigated the transfer of chirality from a molecular motor to a dynamic helical polymer via ionic interactions.[97] A dopant with photoswitchable chirality is able to induce a preferred helicity in a poly(phenylacetylene) polymer and the helicity is inverted upon irradiation. Irradiation at 312 nm of a sample of polymer doped with the (*P*,*P*)-(*Z*)-isomer of the motor resulted in an inversion of the CD signal and hence, the inversion of the handedness of the polymer. In sharp contrast, when a sample of polymer doped with the (*P*,*P*)-(*E*)-isomer of the motor was irradiated, no inversion of the CD signal was observed, only a decrease in intensity in the CD spectrum.

Alternatively, the polymer can respond to the isomerization of embed chiral inductors and consequent alteration of chain coiling with a change of material shape or size, rather than a preferred strand helicity. Depending on the polymer design, an expansion or contraction of the fibers can lead to a three-dimensional rearrangement of the whole structure. These functional materials were shown to be capable of converting light energy into mechanical work at the macroscopic scale, which could lead to potential applications in micromechanical systems, soft robotics and artificial muscles.

Katsonis and co-workers developed liquid-crystal polymer networks that can selectively form either right-handed or left-handed macroscopic helices at room temperature (Figure 1.7).[98] These versatile materials consist of molecular azobenzene-based photochromic switches **12** (Figure 1.7a, concentrations up to 10 wt%) embedded in a liquid-crystalline polyacrylate material containing chiral dopants (Figure 1.7b), resulting in spring-like strings (Figure 1.7c). In these springs, reversible light-induced *trans-cis* isomerization of azobenzene units (λ = 365 nm and >420 nm) is converted and amplified stereospecifically into controlled and reversible twisting motions. Liquid-crystal polymer networks display a strong coupling between orientational order and mechanical strain, which is why they undergo deformations when submitted to a stimulus-induced decrease of order. Upon photoinduced deformation, the springs display complex motion, which includes winding, unwinding and helix inversion, as dictated by their initial shape which in turn depends on the direction in which they are cut (Figure 1.7c). Shape and photo-actuation modes of the polymer springs are in function of the angular offset, which is defined as the angle between the orientation of the molecules at mid-plane and the cutting direction. Under irradiation with ultraviolet light, the ribbons contract along the director and expand in the perpendicular directions, as is consistent with an ultraviolet-induced increase of disorder. The ribbons deform to accommodate the preferred distortion along the main axis of the ribbon, and this preferred distortion is determined by the orientation of the molecules. Importantly, they can produce work by moving a macroscopic object and mimicking mechanical functions such as those used by plant tendrils to help the plant access sunlight.

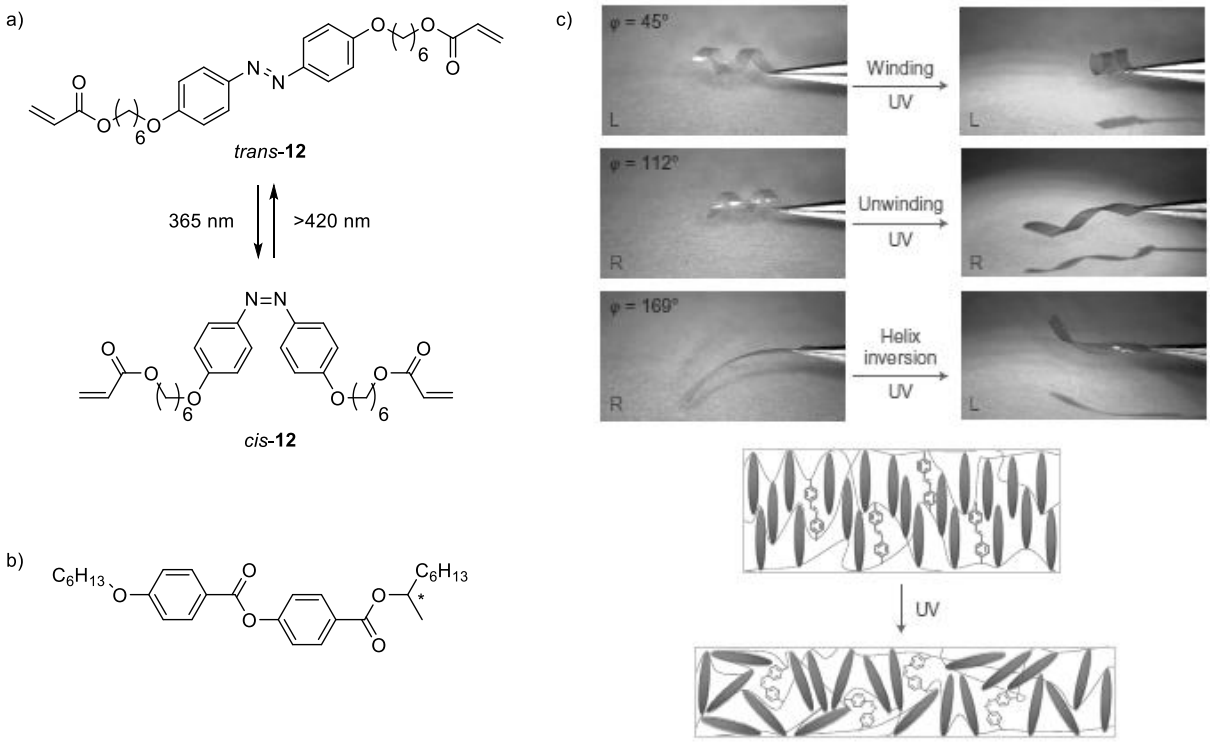

Figure 1.7. Photoresponsive liquid crystal in a twist-nematic molecular organization, as developed by Katsonis and co-workers. a) Photoisomerization process of azobenzene actuator **12**, incorporated in liquid-crystalline polyacrylate springs upon copolymerization. b) Chiral dopants used to induce preferential helicity to the spring. c) Spiral ribbons irradiated for two minutes with ultraviolet light (λ = 365 nm) display isochoric winding, unwinding and helix inversion as dictated by their initial shape and geometry. Reverse motion can be achieved upon irradiation with visible light (λ > 420 nm). Reproduced with permission from Ref. 98.

Giuseppone and co-workers have developed a polymeric gel including second generation overcrowded alkene based molecular motors, which contracts upon irradiation with UV light (Figure 1.8).[99] The polymer motor conjugates consist of fast second generation motors (rotation frequency in the order of MHz) cross-linked with PEG chains. On performing copper-catalyzed azide-alkyne cycloaddition (CuAAC) reactions under high-dilution conditions (Figure 1.8a), 8-shaped macrocyclic motor conjugates **13** are formed (Figure 1.8b). The macrocycles can be coiled up by light activation, thus reducing their size to that of nanoscopic objects which can be identified by AFM as isolated coiled 8-shaped polymers on mica surfaces (Figure 1.8d). When the CuAAC reaction is carried out at much higher concentrations (Figure 1.8a), the result is mechanically activated entangled gels **14** in which the polymer chains become coiled up by the UV-light-activated rotations of the entrapped motors (Figure 1.8c), reducing the overall dimensions of the millimeter-sized gels (Figure 1.8e). It is hypothesized that this shrinking is the result of increasingly tighter coiling of the polymeric chains, induced by the continuous rotation of the motor units. At higher tensions the contraction slows down, until the gel ruptures and subsequently recovers its original size and shape. Complimentary fluorescence experiments indicate that the rupture is the result of simultaneous oxidation of the central double bonds of the motors, followed by unwinding of the coils. Using bidirectional rotating units, one could envision selectively shrinking or expanding the gel structure upon rotation in opposite direction. Therefore, a dynamic transfer of chirality from a specific rotational motion to a consequential three-dimensional size regulation can be recognized. Potential practical applications of such systems may include energy storage, smart materials and artificial muscles.

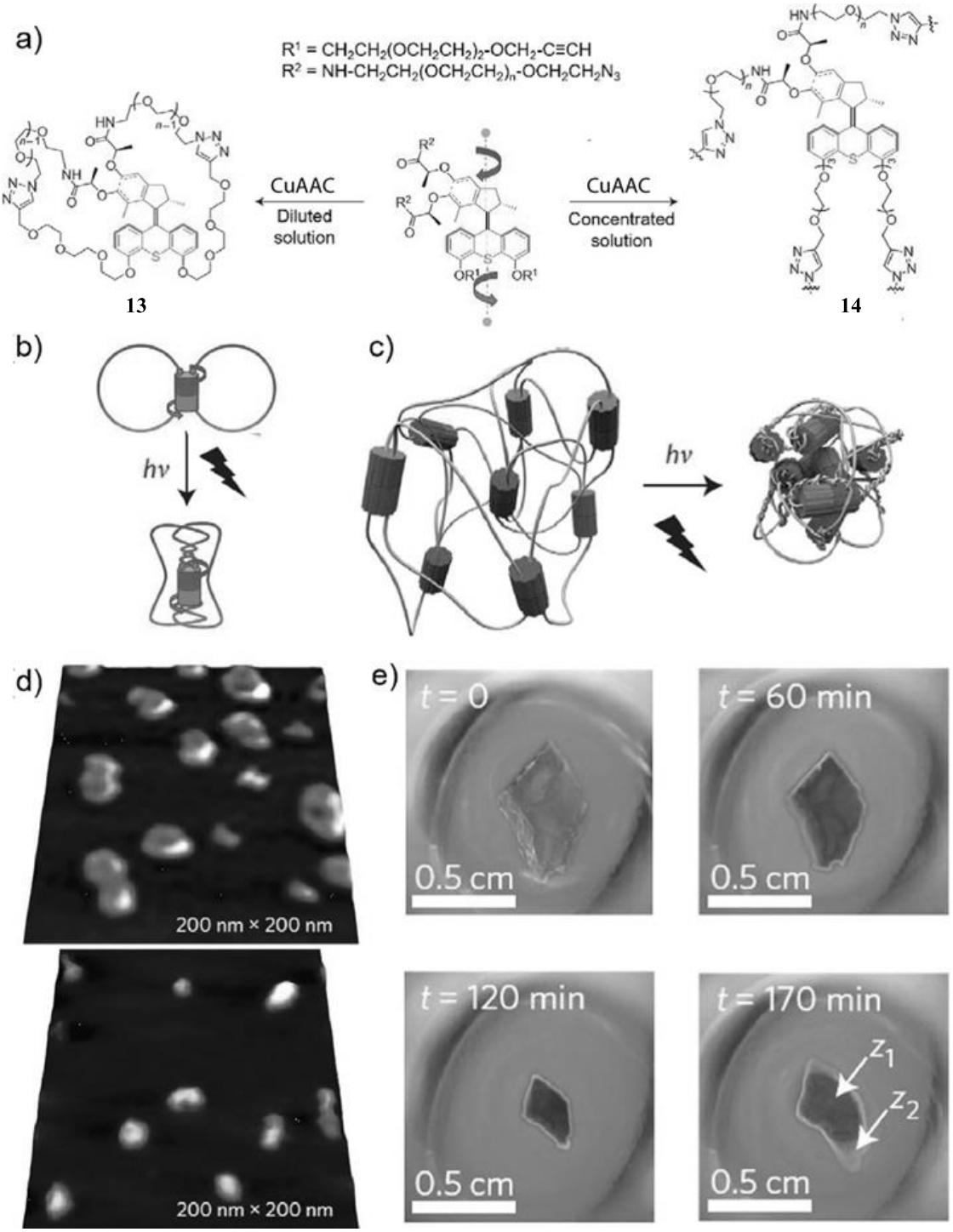

Figure 1.8. Size-reduction of nanoscopic objects **13** and macroscopic entangled gel **14** contractions driven by artificial molecular motors developed by Giuseppone and co-workers. a) Reaction schemes and conditions for incorporating artificial molecular motors into an 8-shaped polymer and into mechanically activated entangled gels. b,c) Graphical illustrations showing the 8-shaped polymer and the mechanically activated entangled gels coiling up under light activation. d) AFM images before (top) and after (bottom) light activation of the 8-shaped polymer. e) Snapshots of a movie (taken at 0, 60, 120, and 170 min after light irradiation, respectively) illustrating macroscopic gel contractions over time. Reproduced with permission from Ref. 99.

The same group also reported that by connecting subunits made of both unidirectional light-driven rotary motors and modulators, which respectively braid and unbraid polymer chains in cross-linked networks, it

becomes possible to reverse their integrated motion at all scales.[100] The photostationary state of the systems can be tuned by modulation of frequencies using two irradiation wavelengths. Under this out-of-equilibrium condition, the global work output (measured as the contraction or expansion of the material) is controlled by the net flux of clockwise and anticlockwise rotations between the motors and the modulators.

1.3.5 Stereoselective catalysis

Enzymes and synthetic asymmetric catalysts exercise tight stereochemical control over the reactions they catalyze, producing, for the most part, single enantiomers. Reversing the chiral preference of a catalytic system is a non-trivial task (for enzymes, directed evolution using genetic engineering has been used).[101] During the last decades, chemists have developed striking examples of reversal of stereoselectivity provided by artificial catalyst by means of externally-induced changes of local chirality.[47,102,103] The use of light to induce a change in catalyst state is particularly attractive as it is non-invasive stimulus, offers excellent temporal and spatial control, and can be precisely regulated with an appropriate light source. In photo-modulated stereoselective catalysis, the stereodynamic properties of chiral photoswitches and their contributions of interconverting configurational and conformational isomers are exploited to achieve control over catalytic selectivity, reactivity, and substrate recognition.[47] In order to proceed at reasonable rate, most catalytic reactions require concentrations that exceed by several orders of magnitude the usual condition employed in photochemistry. However, the use of photoresponsive catalysts allows lowering the concentration of the active chromophore in the reaction mixture.[47] Moreover, the photoswitching of catalytic activity and/or selectivity in facts constitutes an amplification of the light stimulus and chirality, since the information triggered upon light irradiation is amplified towards multiple asymmetric catalytic events.[47] Most of the photoswitchable catalyst systems reported to date focus on the modulation of catalytic activity by triggering a change of the catalyst structure between two forms. Control over cooperative effects,[104–106] competing effect,[107,108] steric shielding of the active site,[109,110] and modulation of pH[111–113] or electronic properties[114,115] are amongst the most relevant and successful approaches.

Much more limited in number and therefore more impressive in their achievements are the examples of photoswitchable catalysts capable of providing selectivity control. The first successful approach to photochemically alter the stereoselectivity of a catalyst was reported by Branda and co-workers (Scheme 1.4).[116] Through cooperative interactions, they successfully controlled the stereochemical outcome of the cyclopropanation of styrene using a photoswitchable chiral copper-based catalyst **15**. Their ligand consists of a dithienylethene-based chiral bis(oxazoline) which, in its open form (**o-15**), binds Cu(I) ions in a bidentate fashion. This results in a rigid chiral environment for the metal ion that subsequently catalyzes the cyclopropanation reaction with significant enantioselectivity (30–50% ee). In contrast, the closed form of the ligand (**c-15**), formed upon irradiation at 313 nm, is only able to form monodentate complexes with Cu(I) due to the rigidity of the ligand. The chiral environment is less well expressed in this complex and results in negligible enantioselectivity in the cyclopropanation reaction (5% ee). Irradiating the sample with visible light led to recovery of the original chiral information and gave an ee of 11–37%. A limitation of this catalytic system is the low photocyclization efficiency in the presence of Cu(I), with only 23% of the closed form present at the photostationary state at 313 nm, meaning that switching the catalyst state only results in a small disruption in the stereoselectivity of the catalyzed reaction.

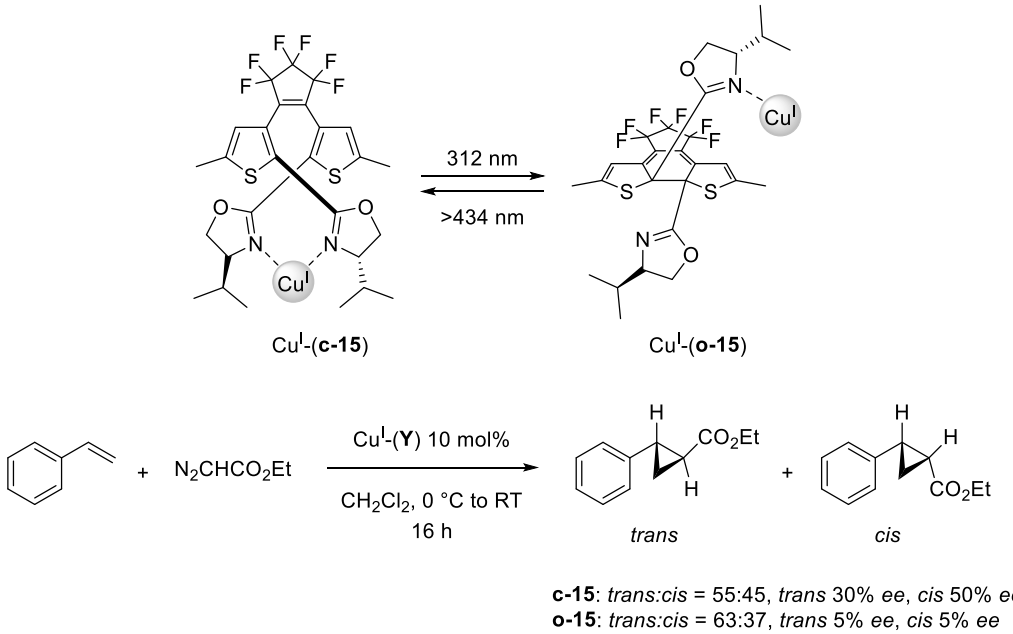

Scheme 1.4. Photoswitching of a dithienylethane-based oxazoline ligand **15** that shows different stereoselectivities in the copper-catalyzed asymmetric cyclopropanation of styrene developed by Branda and co-workers.

Feringa and Wang have risen to the challenge by integrating a catalytic system with a light-driven first generation molecular motor **16**, which allows controlling of catalytic activity and configuration of the product (Figure 1.9a).[117] The motor is functionalized on its rotor segment with a dimethylaminopyridine unit (Brønsted base, A) and on its stator segment with a thiourea function (hydrogen-bond donor, B) that can act cooperatively as a bifunctional catalyst for a conjugate thiol addition to enone (Figure 1.9b). When the motor is activated to undergo photochemically and thermally induced steps, counter-clockwise rotation of the rotor around the overcrowded alkene bond controls the backbone helicity (*M* or *P*) and relative distance the catalytic groups, A and B, producing catalysts ***I***, ***II*** and ***III*** in sequence with different activities (Figure 1.9c) and enantioselectivities (Figure 1.9d). The catalytic system displays low catalytic activity and almost no chiral preference when A and B are far apart (***I***). The catalytic activity is increased significantly when A and B are close together, as in ***II*** and ***III***, while the chiral preference is reversed when the rotor has (*M*) and (*P*) helicities. Indeed, the catalyzed reaction yielded the addition product with different e.r. and yield (comparison after 15 h) upon tuning of the catalyst, going from *R*:*S* = 51:49 and 7% yield (***I***), to *R*:*S* = 25:75and 50% yield (***II***), and *R*:*S* = 77:23 and 83% yield (***III***). The concept of application molecular motors in photoresponsive stereoselective catalysis was further extended by Vlatkovic to an analogous dimethylaminopyridine-thiourea functionalized organocatalysts **17** to control a Henry reaction[118] (Figure 1.10a) and by Zhao to a bis(diphenylphosphine) ligand **18** for palladium-catalyzed enantioselective allylic substitution (Figure 1.10b).[119]

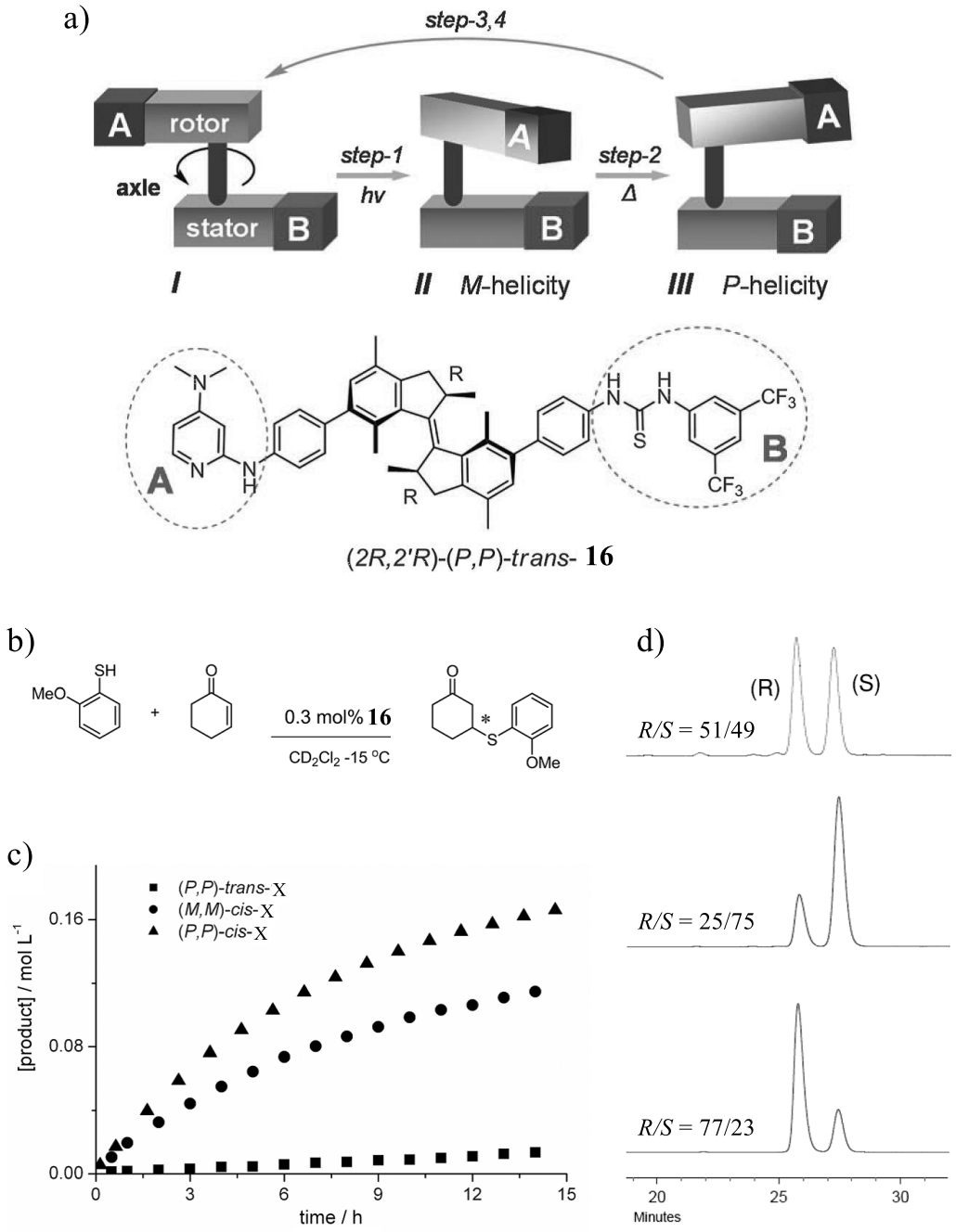

Figure 1.9. Reversal of enantioselectivity controlled by a unidirectional rotary motor **16** by Feringa and co-workers. a) Graphical representation of the motor motion (top) and structural formula of the artificial switchable catalyst in its (2*R*,2'*R*)-(*P*,*P*)-*trans* form (bottom). **A** and **B** stand for the rotor and stator components, respectively. Unidirectional step-wise rotation around central alkene leads to the molecule adopting three geometries, namely, ***I***, ***II***, and ***III***, with different catalytic performances. b) Reaction Scheme 1.and conditions for the thiol addition to enone catalyzed by **16**. c) Reaction kinetics by ^{1}H NMR spectroscopy show that the motor functions effectively only when portion A and B are close enough in its (*M*,*M*)-*cis* form (***II***) and (*P*,*P*)-*cis* form (***III***). d) Chiral HPLC traces illustrate the variation of enantioselectivity upon catalyst isomerization (catalyst form, e.r. *R*:*S* of reaction product: ***I***, 51:49; ***II***, 25:75; ***III***, 77:23, from top to bottom, respectively). Reproduced with permission from Ref. 117.

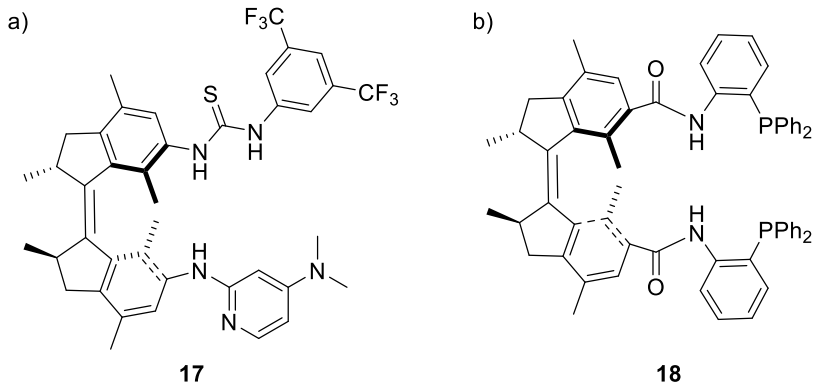

Figure 1.10. Bifunctional first generation molecular motor derivatives **17** and **18** for stimuli-responsive control of catalytic activity and enantioselectivity in organo- and metal-catalyzed transformations: a) Henry reaction;[118] b) Palladium-catalyzed enantioselective allylic substitution.[119]

Chen and co-workers reported a pseudo-enantiomeric pair of optically switchable helicenes **19** composed of a C2-symmetric dimethoxymethyl-dibenzosuberane stator and a catalytic 4-*N*-methylaminopyridine (MAP) rotor joined by a switchable olefin (Figure 1.11).[120] They underwent complementary photoswitching at with UV-light (*P*:*M*, <1:>99 at 290 nm; 91:9 at 340 nm) and unidirectional thermal relaxation similarly to the helicenes previously described by the same group (see Figure 1.4). They were utilized to catalyze enantiodivergent Steglich rearrangement of O- to C-carboxylazlactones, with formation of either enantiomer with up to 91% ee (*R*) and 94% ee (*S*), respectively. Based on control experiments, the authors proposed that the catalytic process may proceed through an initial and reversible nucleophilic carboxyl substitution of the substrate carbonate moiety by catalyst, resulting in the formation of a stabilized ion pair (*P*)-**19'** between the enolate-anion of the substrate and phenoxycarbonyl-pyridinium-cation of the catalyst. Subsequently, an irreversible C-carboxylation of enolate-anion takes place with pyridinium-cation in high enantiocontrol.

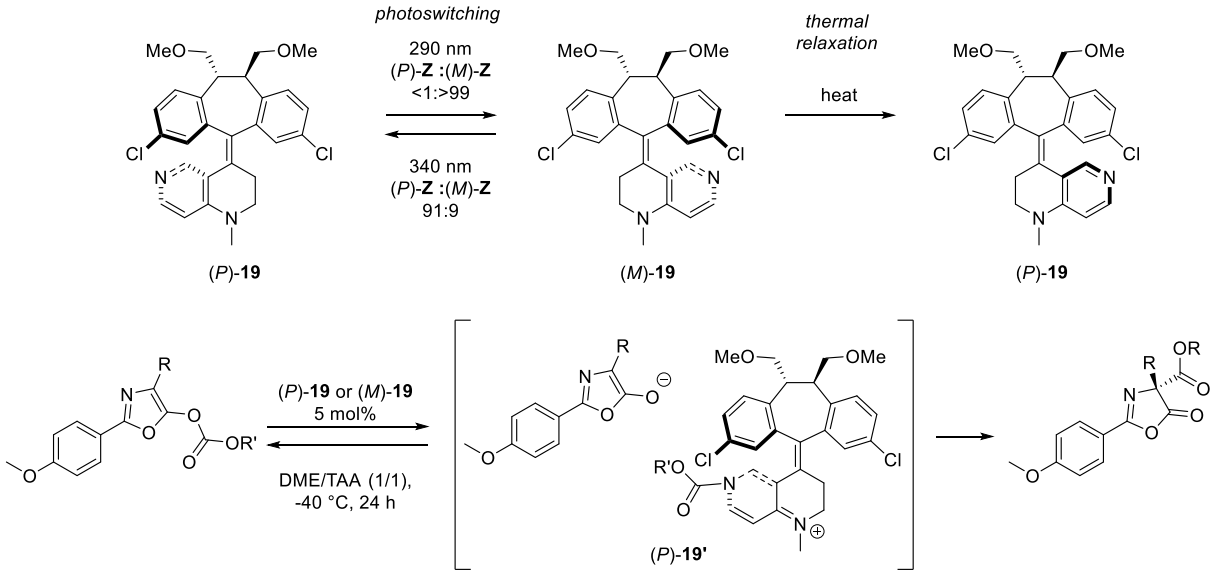

Figure 1.11. Photoisomerization profiles of catalytic C_2-symmetric dibenzosuberane-based helicenes **19** for the stereoselective Steglich rearrangement of O-carboxylazlactone developed by Chen and co-workers.

1.3.6 Host-guest interaction and chiral recognition

The vast majority of biomolecules is chiral and the ability of proteins to distinguish between enantiomers is of fundamental importance to various biological processes, for example, signal transduction, drug binding, and biocatalysis.[121] Consequently, chemists have been highly active in the area of chiral recognition and especially enantioselective discrimination.[122,123] In principle, the enantiopreference of any biological or chemical receptor is fixed by the chiral building blocks that it is made from. Yet, it is intriguing to develop chirality-switchable receptors that could selectively bind a given enantiomer in one state, whereas in the other state it prefers binding the opposite enantiomer. Such receptors could be used to dynamically control the ratio between enantiomers or selectively transport an enantiomer of choice. Knowing that opposite enantiomers of chiral substrates can produce entirely different effects,[124] this may be applied eventually also to exert unique control over chirality-responsive biological and chemical processes.

Aida and co-workers designed a chiral photoresponsive host **20** capable of light-induced scissor-like conformational changes (Scheme 1.5).[125] The system can give rise to mechanical twisting of a non-covalently bound bidentate guest rotor molecule. To realize this coupling of molecular motions, they uses a previously designed system:[126] a ferrocene moiety with an azobenzene strap, each end of which is attached to one of the two cyclopentadienyl rings of the ferrocene unit, acts as a pivot so that photoisomerization of the strap rotates the ferrocene rings relative to each other and thereby also changes the relative position of two 'pedal' moieties attached to the ferrocene rings. This effect is translated into intermolecular coupling of motion by endowing the pedals with binding sites, which allow the host system to form a stable complex with a 4,4'-biisoquinoline guest **21**. Exposure of *trans*-**20** to UV light (λ = 350 nm) at 20 °C induces *trans*-*cis* isomerization of the azobenzene unit to give a molar ratio for *trans*-**20**:*cis*-**20** of 22:78. Irradiation of the isomerized mixture with visible light (λ = 420 nm) resulted in the backward *cis*-*trans* isomerization, giving a molar ratio for *trans*-**20**:*cis*-**20** of 63:37. Using circular dichroism spectroscopy, they demonstrated that the photoinduced conformational changes of the host are indeed transmitted and induce mechanical twisting of the rotor molecule.

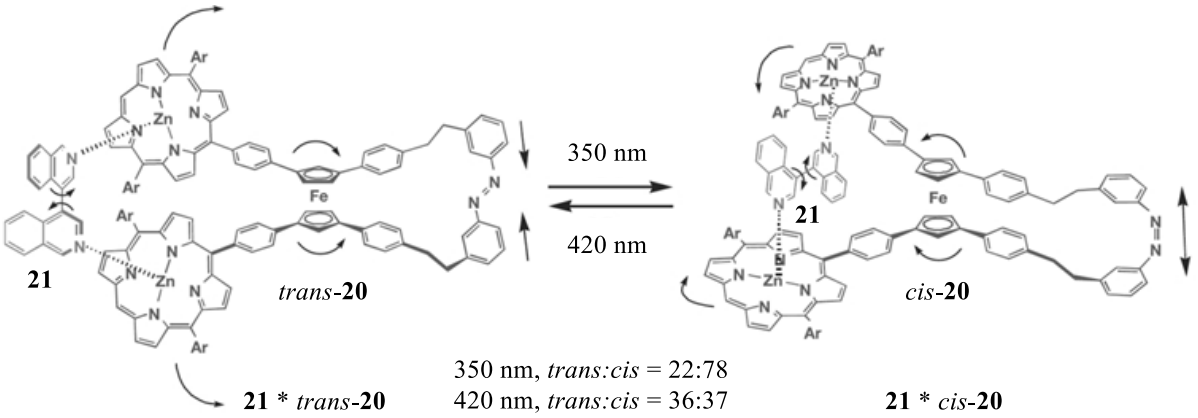

Scheme 1.5. Schematic representation of light-powered molecular pedal **20** capable of inducing conformational changes via host-guest interaction, developed by Aida and co-workers. Reproduced with permission from Ref. 125.

Feringa, Wezenberg and co-workers reported a chiral bis-urea anion receptor **22**, derived from a first generation molecular motor, which can undergo photochemical and thermal isomerization operating as a reconfigurable system (Scheme 1.6).[127] The two possible *cis* configurations in the isomerization cycle are opposite in helicity. They demonstrated that the (*P*)- and (*M*)-helical *cis*-isomers hold opposite enantioselectivity in the binding of BINOL phosphate, while anion complexation by the intermediate *trans*-isomer is not selective. Thus, the enantio-preferred substrate binding in this receptor can be inverted in a dynamic fashion using light and heat. Irradiation of a solution of stable (*P*,*P*)-cis-**22** with UV-light (λ = 312 nm) resulted, via generation of (*P*,*P*)-*trans*-**22** isomer as intermediate, in conversion to (*M*,*M*)-*cis*-**22**.

Upon subsequent heating of the sample, regeneration of the initial stable (*P*,*P*)-cis-**22** was observed. Fitting of the ^{1}H NMR spectroscopy titration data of a sample of (*P*,*P*)-*trans*-**22** and $[Bu_4N]^+[(R)\text{-}\mathbf{23}]^-$ or $[Bu_4N]^+[(S)\text{-}\mathbf{23}]^-$ to a 1:1 binding model revealed a strong preference for binding of the (*R*)-enantiomer over the (*S*)-enantiomer ($K_R/K_S = 4.2$). To determine a stability constant for complexation of **23** by (*M*,*M*)-*cis*-**22**, competitive titrations to the photostationary state (at $\lambda = 312$ nm) mixture (PSS_{312}: *cis*:*trans* = 80:20) were carried out under the same conditions. It was found that now the (*S*)-enantiomer of **23** binds the strongest ($K_R/K_S = 3.2$). However, in addition to stereoselective inversion, a decrease in binding strength was noted when going from (*P*,*P*)-*cis*-**23** to (*M*,*M*)-*cis*-**23**. On the other hand, titrations to (*P*,*P*)-*trans*-**23** revealed poor binding ($K_a < 20\ M^{-1}$) and no enantioselectivity. Binding tests with more sterically hindered guest **24** displayed less efficient enantiodiscriminating performances.

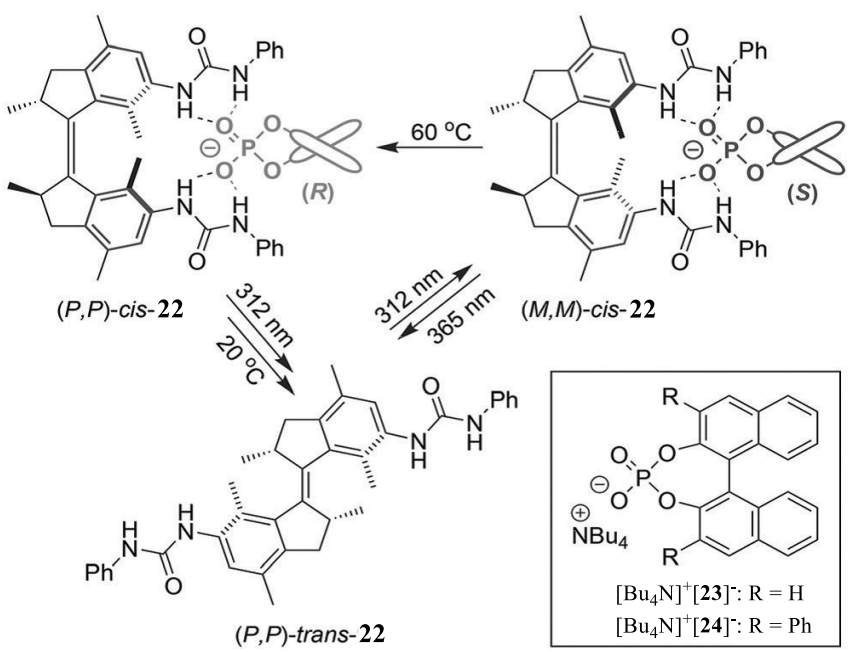

Scheme 1.6. Schematic representation of bis-urea receptor **22** controlled by light and heat for dynamic inversion of stereoselective phosphate binding developed by Feringa and co-workers. Reproduced with permission from Ref. 127.

Dynamic control over helicity of chiral metal-ligand complexes has also been described. Taking inspiration from Cu-helicates by Lehn and others,[128,129] Feringa, Zhao and co-workers reported that unidirectional rotary motors with connecting oligo-bipyridyl ligands **25** and **26** (Figure 1.12a), which can dynamically change their chirality upon irradiation, assemble into metal helicates that are responsive to light.[130] The motor function controls the self-assembly process as well as the helical chirality, allowing switching between oligomers and double-stranded helicates with distinct handedness (Figure 1.12b). Coordination oligomers of bipyridine-Cu(I) complex can be formed by treating the *trans*-molecular motor bearing oligobipyridines with Cu(I). These oligomers can split into monomers with *P'*-helicity due to the unidirectional rotation of the molecular motor from the stable (*P*,*P*)-*trans*-state to the metastable (*M*,*M*)-*cis*-state with light. Analysis by UV–vis, CD and ^{1}H NMR spectroscopy demonstrated that the inversion of the chirality of the Cu-helicate from *P'* to *M'* is governed by a subsequent thermal helical inversion [from (*M*,*M*) to (*P*,*P*)] of the molecular motor core structure. Photoisomerization of stable (*P*,*P*)-*cis*-state to stable (*M*,*M*)-*cis*-state through the rotary cycle via the metastable *trans*-oligomeric-state will invert the chirality of the Cu-helicate back from *M'* to *P'*. In this system, the achiral guests (i.e. the Cu(I) ions) support the chiral photoresponsive selector to construct out of the polydentate ligand strands a supramolecular helical structure with dynamic helicity. The unidirectionality of the light-induced motion governs the sequence of programmable steps, enabling the highly regulated self-assembly of fully responsive helical structures.

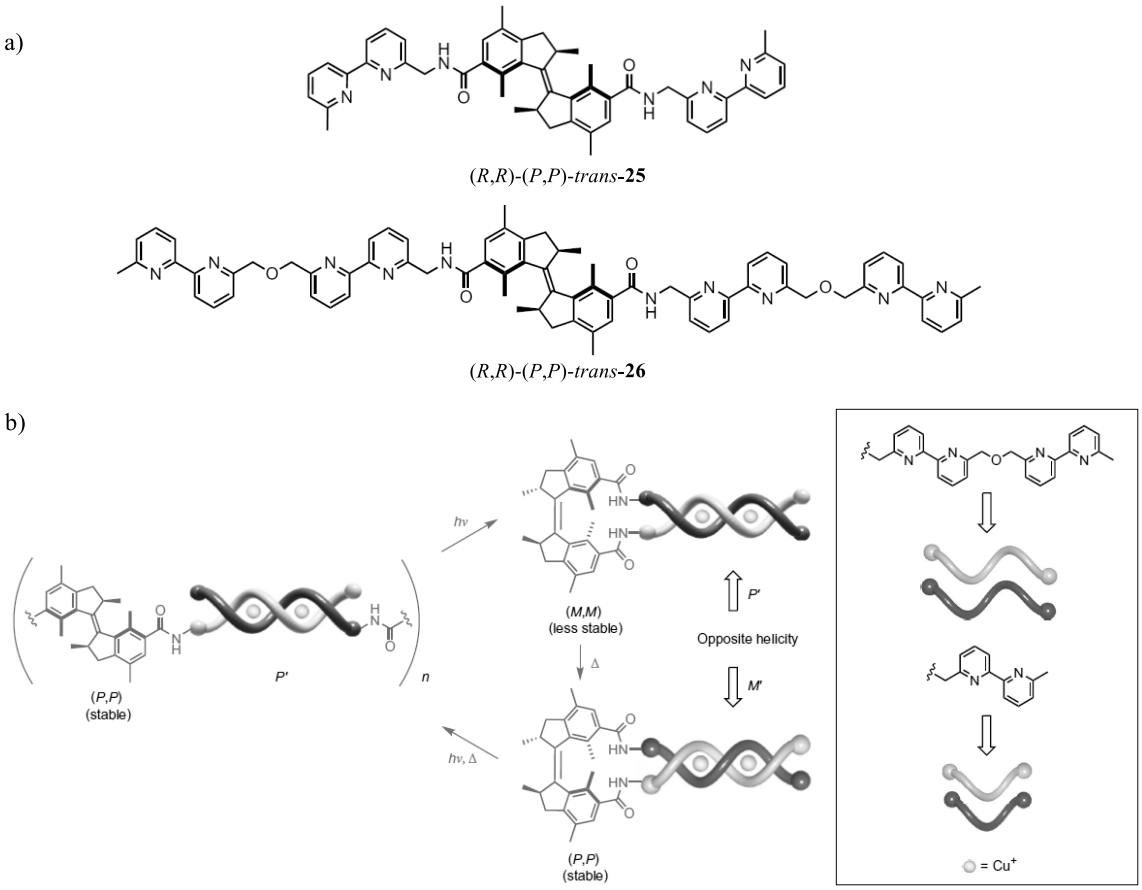

Figure 1.12. Dynamic control of chirality and self-assembly of double-stranded helicates **25** and **26** with light and heat developed by Feringa and co-workers. a) First generation molecular motors bearing oligobipyridines ligand strands **25** and **26**. b) Schematic representation of the concept of the dynamic double-stranded helicates with coordinated Cu(I) ions. Reproduced with permission from Ref. 130.

1.3.7 Photocontrol of biological systems

The ability to control the conformation and activity of biomolecules in a reversible manner is a fascinating goal[48,131–133] that has an outstanding potential for the study of and interference with complex processes in living cells.[134,135] Spatial and temporal control of cellular processes could provide unparalleled opportunities for elucidating biological events or disease progression.[136,137] Light is considered an ideal external control element for *in situ* chemical and biological manipulation because it offers a high level of spatio-temporal resolution, its energy and intensity can be precisely regulated, is generally non-invasive within specific a range of wavelengths, is orthogonal toward most elements of living systems, and does not cause the chemical contamination of the sample.[138] Many strategies for the reversible photocontrol of biomolecules have been explored with a wide variety of chromophores. A promising approach along this line features site-specific anchoring or chain-insertion of a photoswitch onto a target protein, peptide or DNA structure. The photoinduced isomerization between the *cis*- and *trans*-isomers (e.g. azobenzenes, overcrowded alkenes) or interconversion between closed and open forms (e.g. spiropyrans, dithienylethenes) results in a net change in geometry, polarity or charge distribution of the chromophore. Examples of photo-regulation of DNA structure[139] and conformation,[140] ligand binding to nuclei acids,[141] peptide conformation[142,143] and functional protein structure and folding (e.g. for control of receptors function,[144] enzyme activity,[145–147] ion channel,[148] and ligand binding[149]) have been reported. It should be noted that most of these examples imply reversible interaction of chiral biological molecules with photoresponsive motifs not characterized by enantioselective switching mechanisms, like azobenzenes or dithienylethenes. The concept of dynamic transfer of chirality is therefore not easy to delineate in this field,

as most systems entail up-down regulation of biological processes by inclusion of artificial photo-actuators without any clear reversal of chiral outcome.[150] For instance, various groups have used light to alter the structure and binding properties of nucleic acids and nucleic acid analogs by employing photochromic molecules introduced in diverse structural positions, including the phosphate backbone, the nucleobase, and ribose moiety in native nucleic acids.[48] The resulting photosensitive oligomers have allowed, for instance, the initiation or inhibition of nucleic acid hybridization simply by using the proper wavelength of light. However, photoinduced destabilization and interconversion of inherently chiral biological structures do involve dynamic interactions between chiral elements.[151] For example, peptides are known to be good synthetic analogs of protein motifs and can exist in disordered or regularly folded structures, such as random-coil, β-sheet, and α-helix structures, depending on reaction medium, pH, and temperature.[152] Incorporating photoresponsive amino acid residues into peptide structures allows for photochemical control of molecular recognition and organization. Some of the most remarkable examples will be described herein. Due to the large number of articles on analogous concepts and approaches, we refer to specialized comprehensive reviews for further details.[48,131–133]

Woolley and co-workers achieved photocontrol over α-helix folding by introducing two cysteine (Cys) residues into peptides and cross-linking these with a photoresponsive bridging unit, an iodoacetamide-modified azobenzene **27** (Figure 1.13a).[153] The distance of the cysteine residues at *i, i+7* spacing was designed to match the linker length of the switch in the *cis*-conformation (Figure 1.13b). As indicated by CD measurements, the isomerization of the azobenzene switch from the *trans-cis* configuration increased helical content from 12% to 48% (Figure 1.13d). Alternative Cys spacing was also investigated in this study. Peptides with alternative spacing *i, i+11* (Figure 1.13c) showed the reverse behavior , with significant helical content for the *trans* isomer (66%).[154]

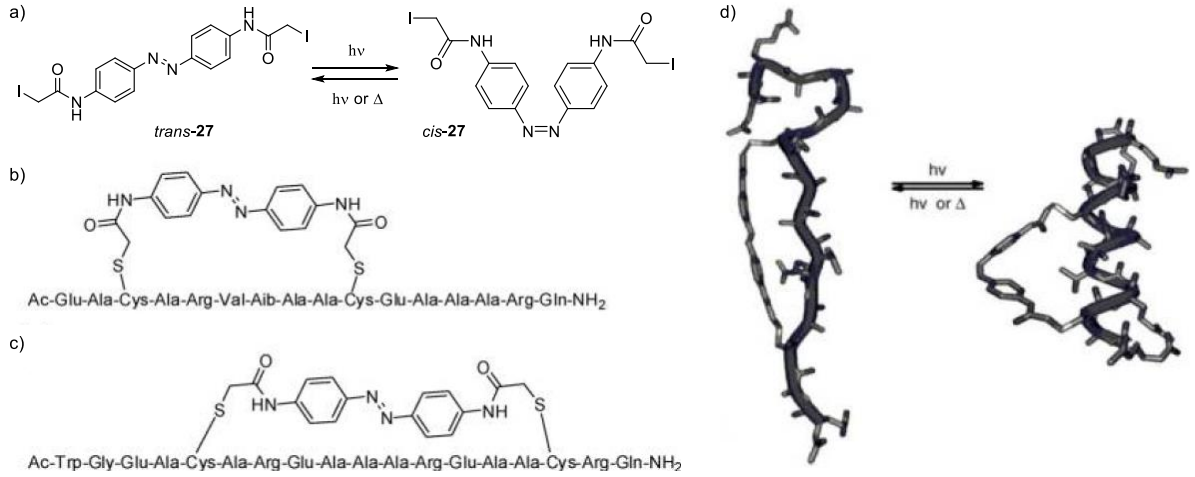

Figure 1.13. Photo-control of helix content in a short peptide reported by Woolley and co-workers. a) Photisomerization of iodoacetamide-modified azobenzene linker **27**. Primary sequences of the cross-linked peptides: b) azobenzene reacted via Cys residues spaced *i, i+7*; c) azobenzene via Cys residues spaced *i, i+11*. d) Model showing the increased helicity induced in the peptide upon *trans-cis* isomerization of the attached azobenzene cross-linker. Reproduced with permission from Ref. 154.

Moroder and co-workers demonstrated photoresponsive folding and unfolding of triple-helix structures in collagen model peptides (Figure 1.14). In the initial approach,[155] mercaptoproline residues were incorporated in the sequence and cross-linked with an azobenzene chromophore **28** (Figure 1.14a). *Trans-cis* isomerization at ambient temperatures unfolded or distorted the triple-helix structure, and thermal relaxation induced refolding (Figure 1.14b). Subsequently, a different approach related to Woolley's was used to cross-link the peptide sequence with the azobenzene chromophore. Unfolding in response to photoinduced isomerization of the triple helix was limited and only observed in the region spanned by the azobenzene switch.[156]

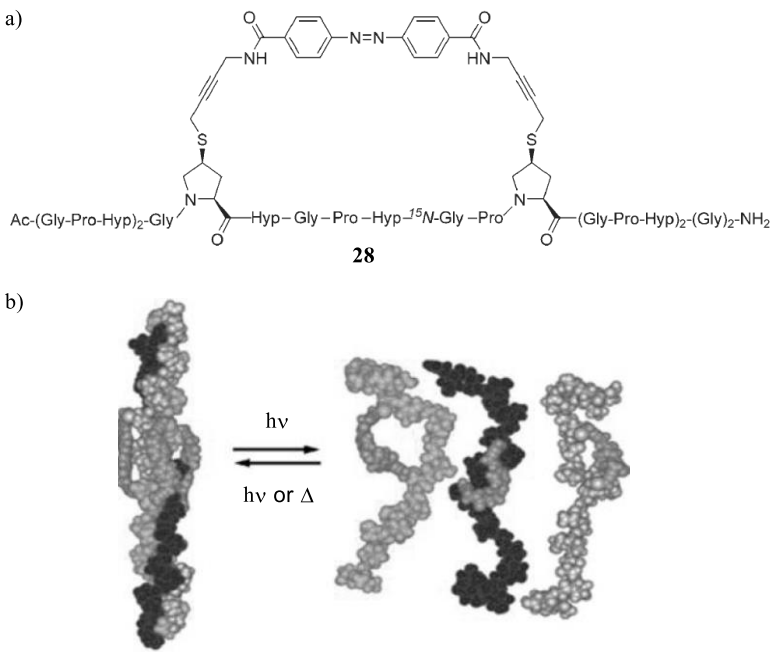

Figure 1.14. Schematic illustration of the unfolding/distortion of triple-helix structure upon *trans-cis* isomerization of cross-linked azobenzene actuator **28** reported by Moroder and co-workers. Reproduced with permission from Ref. 155.

Clayden and co-workers reported the conformational photoswitching of a synthetic peptide foldamer **29** bound within a phospholipid bilayer akin to a biological membrane phase (Scheme 1.7).[143] The described photoswitchable helical molecules contain an azobenzene unit, which could be tuned with appropriate substituents to affect its switching performances and bi-stability. The chromophore is attached to a helical oligoamide that both promotes membrane insertion and communicates conformational change along its length. Isomerization of the initial *E*-form could be achieved selectively and reversibly (λ = 365 nm, *E*:*Z* up to 14:86; λ = 455 nm, *E*:*Z* up to 71:29). Light-induced structural changes in the chromophore are translated into global conformational changes, which propagate over several nanometers within a membrane environment through helical structures with selectable twisting-sense. Upon sequence of irradiation, the population distribution of the peptide helixes varied from the initial left-handed helicity (dark), to a large extent of right-handed form (λ = 365 nm) with up to 66% of the equilibrium population, and back to original left-handed form (λ = 455 nm).

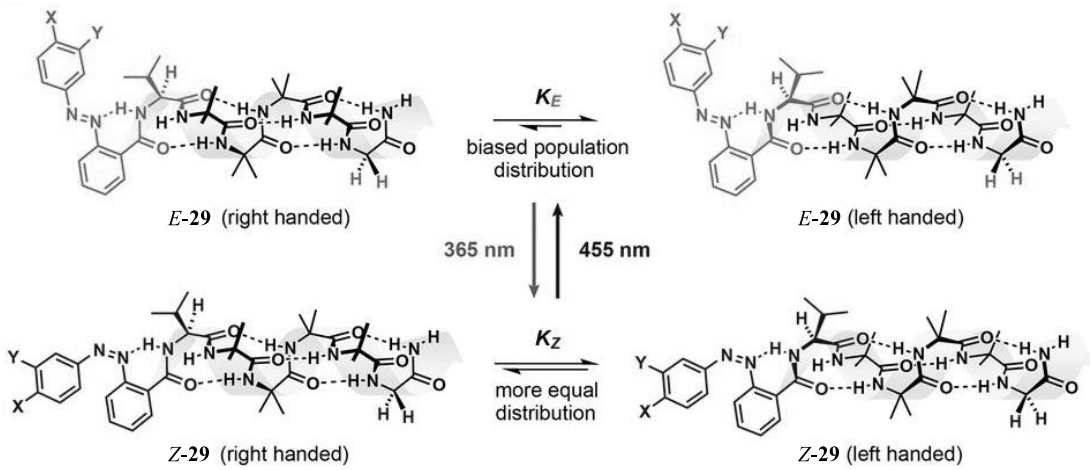

Scheme 1.7. Conformational photoswitching of a synthetic peptide foldamer **29** bound within a phospholipid bilayer, as described by Clayden and co-workers. Reproduced with permission from Ref. 143.

Feringa, Poloni and co-workers described the use of a first generation molecular motor to control a model β-hairpin peptide.[157] Photoswitchable β-hairpins are also considered for their ability to form hydrogels: they can be useful in tissue engineering, drug delivery and biosensing.[158] Simple β-hairpins, bearing an azobenzene unit, have been used to modulate viscoelasticity of a peptide hydrogel.[158] Notably, the light- and heat-responsive unit in **30** undergoes a large conformational change between a thermally stable *trans*-isomer (stable *trans*-**30**) and two thermally bi-stable *cis*-isomers featuring opposite helicity (metastable *cis*-**30** and stable *cis*-**30**) (Scheme 1.8). This dynamic chiral induction has major influence on the secondary structure and the aggregation of the peptide, permitting the photo-triggered formation of amyloid-like fibrils. The β-hairpin sequence used in this design is called trpzip. The trpzips are stable β-hairpins which fold in a monomeric form without requiring metal binding, due to the stabilization by cross-strand pairs of indole rings.[159] The switching properties of **30** were investigated in methanol and water, using HPLC, CD, UV-vis and NMR spectroscopy. The irradiation of stable *trans*-**30** to metastable *cis*-**30** afforded photostationary state of 7:93, respectively. Subsequent thermal isomerization of metastable *cis*-**30** yielded stable *cis*-**30**, was achieved at 40–50 °C within 6 h. Inversion of supramolecular helicity was suggested upon inversion in CD signal of the band corresponding to interacting indole rings of the β-hairpin. From the in depth analysis, it was concluded that *trans*-**30** does not seem to adopt any secondary structure and exists in a monomeric state. Metastable and stable *cis*-**30** both form aggregates, and the decrease in temperature promotes this process. The aggregation properties were studied by TEM and cryo-TEM, which allowed to identify in each state more than one type of aggregate (sheet-like structures, vesicles and fibers), which is the characteristic behavior of peptides adopting a β-hairpin structure. Additionally, some of the aggregate could be disrupted by irradiation.

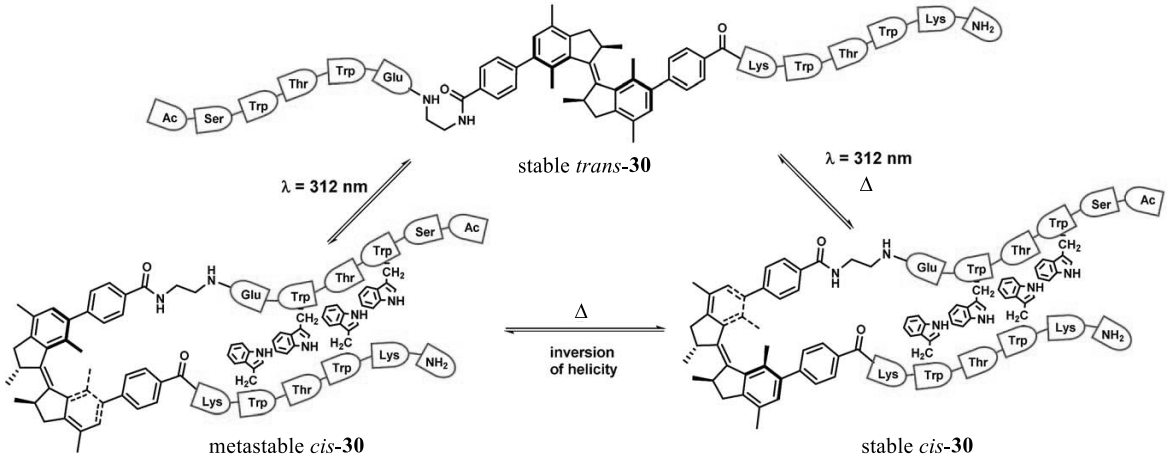

Scheme 1.8. Light and heat control over secondary structure of an overcrowded-alkene-modified Trp zipper **30**, as described by Feringa and co-workers. Reproduced with permission from Ref. 157.

1.4 Conclusions

The complex interplay between the fixed chirality and flexible chirality embedded within the components of (supra)molecular assemblies has given access to a playground full of remarkable nanosystems capable of displaying controllable dynamic transfer and amplification of chirality. Among the several described approaches exploited to achieve external control over responsive molecular systems, this chapter focuses on the use of light as non-invasive input to drive asymmetric responses by photoisomerization of embedded chiral molecular switches or motors. Most remarkable examples are based on sterically overcrowded alkenes, azobenzenes and dithienylethenes derivatives that confer helix inversion and motion capabilities to nanovehicles, liquid crystals, polymers, gelators, catalysts, and biological derivatives. The exponential increase in examples showing amplification of chirality in covalent and supramolecular systems over the last decade may eventually lead to an increased understanding of the factors responsible for the delicate

chiral interplay. However, the detailed studies over chirality transfer and amplification in dynamic photoresponsive systems have also highlighted many critical factors, such as light-induced decomposition, limited penetration depth and wavelength window of irradiating light, excitation/inhibition of neighboring chromophores, sub-optimal switching selectivity, and concentration-dependent balance between overall switching efficiency and asymmetric response. The constant improvement of photochromic switches and their structurally related switching performances is providing chemists with higher precision triggering and more robust tools to finally meet the expectations of diverse applications.[160] As a matter of fact, predicting sensible practical applications of responsive molecular systems is far from being easy at the current state of the art. Based on the overwhelming number of recent reviews on responsive molecular switches and nanosystems,[40,41,54,102] research into wholly synthetic molecular machines appears to have reached a peak point, which culminated with the Noble Prize for Chemistry awarded in 2016.[161] If this point in the rise of molecular machines[162,163] has indeed been reached, then the questions which arise are *what next* and *where next*?[164] Looking back at the history of science, applications which find their way into our everyday lives are a prerequisite for the development of a new field of technology research. With the rise of molecular and cellular biology during the past half century, biologists have led us to believe that, although living systems are extremely complicated, there are strong interdependent relationships between small and large molecules that work in unison to produce, store, and consume energy so that life can be sustained across a wide range of length scales. For just over a couple of decades, chemists have started to design and synthesize wholly synthetic molecules capable of performing some of the tasks of their biological counterparts.[38] Thus far, the greatest obstacle of nanomachines has been to overcome Brownian motion,[165,166] for which cooperation of multiple responsive units and chiral amplification towards adaptable supramolecular systems are likely to be an important strategy. Careful planning ought to be dedicated to the matters of length scales, robustness, reproducibility and efficiency. It would seem to us that, although there is surely room to go in search of applications across all length scales, we do need to devote much more time and effort in working out how to harness and amplify the output of molecular motors operating collectively and efficiently away from equilibrium[167] in robust settings within sustainable surroundings.[168,169] Once again, Nature inspires scientists by providing an excellent example. One of them is the ability of fire ants (*Solenopsis Invicta*) to construct bridges, rafts and even temporary shelters using their own bodies as building material, with no main head in charge and through a continuous reorganization of their structure to maintain stability.[170] Much more complex in design and high-aimed target is the treatment of illnesses and dysfunctions, often regarded as one the long-term goals of nanotechnology when applied to medicine. The importance of this subject cannot be underestimated. After all, the concept of nanotechnology and nanorobots have in fact found place in plenty of science fiction book and movies for more than half a century,[171] providing bright ideas for real applied research groups to dream and work on. After giving our personal contribute to this field, I can safely say that my young colleagues of the Feringa molecular machines research group and myself cannot wait to see it come true.

1.5 Aim and outline of the thesis

The work described in this thesis explores how of second generation molecular motors/switches can be tuned, modified and applied in photoswitchable catalysis. The final aim is to develop alternative designs of switchable catalysts which could display improved thermal stability and more advanced catalytic performance when compared with previously described systems based on first generation molecular motors. We envisioned these novel responsive scaffolds to be tailored for applications via multiple modes of catalytic activity (e.g. metal-catalysis, organocatalysis, activity control, dual stereocontrol) and in wider range of reaction conditions (e.g. temperature, reaction time). Particular attention was dedicated to the development of stereoselective catalytic systems, harnessing the distinctive switchable helicity of molecular motors via dynamic transfer of chirality. Conventional classes of photochromic molecules, such as azobenzenes, spiropyrans and dithienylethens, are not suited for such applications, as they cannot provide a strong and reversible enantiomorphous induction upon photoswitching. Moreover, the characteristic structure of second generation molecular motors was also hypothesized to be a promising candidate for the

development of the first trifunctionalized switchable catalyst featuring two orthogonal catalytic sites for application in light-assisted tandem catalysis. Such systems could ensure high spatio-temporal control of catalytic functions by means of non-invasive input, improving the catalyst efficiency and reducing the number of purification steps required in multi-step synthesis. An example of ultimate application of stereoselective switchable catalysis could the industrial production of polymers with tailored tacticity, on which their physical and mechanical properties are highly dependent. However, the systems and properties disclosed in this work hold great promises also for other applications in the wide field of smart materials, in particular where dynamic control of chirality could provide superior control of chemical functions and molecular architecture. Important aspects that will hereby be addressed are how certain modifications to the molecular structure affects the photochemical behavior and thermal stability of metastable species, and which catalytically active functions are successfully implemented in chiral tunable catalyst based on overcrowded alkenes.

Chapter 2 describes the synthesis of four chiral overcrowded alkenes and the experimental and computational study of their photochemical and thermal behavior. Kinetic studies on metastable isomers using CD spectroscopy and HPLC analysis revealed two pathways at higher temperatures for the thermal relaxation, namely thermal *E*–*Z* isomerization (TEZI) and a thermal helix inversion (THI). Overall, the alkenes studied showed a remarkable and unprecedented combination of switching properties including dynamic helicity, reversibility, selectivity, fatigue resistance, and thermal bistability. The switches described herein have been used as central switchable units for the development of various photoresponsive catalysts in the following chapters.

Chapter 3 focuses on the development of two bifunctionalized molecular switches featuring a thiourea substituent as hydrogen-donor moiety in the upper half and a basic dimethylamine group in the lower half. This combination of functional groups offers the possibility for application of these molecules in photoswitchable organocatalytic processes. Control of catalytic activity in the Michael addition reaction between (*E*)-3-bromo-β-nitrostyrene and 2,4-pentanedione is achieved upon irradiation to the metastable state, providing systems with the potential to be applied as ON/OFF catalytic photoswitches.

Chapter 4 describes the study towards a trifunctionalized molecular photoswitch based on an overcrowded alkene for light-assisted tandem catalytic processes. We proposed a two-step sequence of Morita–Baylis–Hillman (MBH) reaction and enamine catalyzed aldol reaction by merging two pairs of orthogonal bifunctional catalytic groups. Alternative designs aimed to improve the catalytic activity in the MBH reaction and related attempted syntheses are presented. Lastly, screening of other transformations that could be mediated by the initially proposed photoswitchable catalysts design is reported.

Chapter 5 presents the synthesis and characterization of a photoresponsive chiral 2,2'-bisphenol-substituted molecular switch, exhibiting a dynamic central-helical-axial transfer of chirality. The potential for dynamic control of axial chirality was demonstrated by its use as switchable catalyst to control the stereochemical outcome of the enantioselective addition of diethylzinc to aromatic aldehydes, with successful reversal of enantioselectivity for several substrates.

In Chapter 6 we demonstrate that photoresponsive phosphoramidite ligands based on the chiral light-driven biaryl-substituted molecular described in Chapter 5 can be used to alter the activity and invert the stereoselectivity of a copper-catalyzed asymmetric conjugate addition. The derivatives were obtained as a mixture of diastereoisomers, each displaying a distinctive catalytic activity and opposite stereoselectivity. The result is an elegant balance of two competing catalysts, of which the complementary catalytic performance is tunable via internal dynamic transfer of chirality upon alkene photoisomerization.

Chapter 7 describes the study towards the synthesis and application of a photoswitchable chiral phosphoric acid based on a second generation molecular motor core. Direct derivatization of the 2,2'-bisphenol-derived chiral molecular switch described in Chapter 5 provided the target compound. The potential for application of the chiral phosphoric acid as switchable organocatalyst in asymmetric transformations was investigated. In order to increase catalytic activity and stereoselectivity, derivatization of the original biphenyl unit design was attempted.

Chapter 8 describes the study towards the synthesis and application of a photoswitchable chiral bis(diphenylphosphine)-ligand upon derivatization of the 2,2'-bisphenol-functionalized chiral molecular switch described in Chapter 5. We envisioned a large variation of axial chiral induction and steric hindrance provided around the coordinated metal center upon photochemical isomerization of the responsive ligand. Several metal-catalyzed aryl phosphination methodologies previously developed for conventional biaryl scaffolds were attempted during the synthesis of the novel photoswitchable ligand. Experimental evidence suggests that the highly hindered structure of the designed bidentate ligand may even preclude the proposed synthetic route at all. An alternative proposal to develop a photoswitchable Brønsted acid catalyst based on an analogous diphenylphosphine-hydroxyl derivative is presented.

1.6 References

(1) Kauffman, G. B.; Myers, R. D. *J. Chem. Educ.* **1975**, *52*, 777.
(2) Grossman, R. B. *J. Chem. Educ.* **1989**, *1*, 30–33.
(3) Eliel, E. L.; Wilen, S. H. *Stereochemistry of organic compounds*; Wiley: New York, **1994**.
(4) Mislow, K. *Introduction to Stereochemistry*; Dover Publications: Dover, **2003**.
(5) Yamamoto, H.; Carreira, E. M. *Comprehensive chirality*; Elsevier Science: Oxford, **2012**.
(6) Bentley, R. In *Encyclopedia of Molecular Cell Biology and Molecular Medicine*; Wiley-VCH Verlag GmbH & Co. KGaA: Weinheim, Germany, **2006**.
(7) Gibney, E. *Force of nature gave life its asymmetry*, http://www.nature.com/doifinder/10.1038/nature.2014.15995.
(8) Mason, S. *Trends Pharmacol. Sci.* **1986**, *7*, 20–23.
(9) Palczewski, K. *J. Biol. Chem.* **2012**, *287*, 1612–1619.
(10) Brown, G. H. *Photochromism*; Wiley-Interscience: New York, **1971**.
(11) Durr, H.; Bouass-Laurent, H. *Photochromism: Molecules and Systems*; Elsevier: Amsterdam, **2003**.
(12) Feringa, B. L.; Browne, W. R. *Molecular Switches Vol. I, II*; Wiley-VCH Verlag GmbH & Co. KGaA: Weinheim, Germany, **2011**.
(13) Feringa, B. L.; van Delden, R. A.; Koumura, N.; Geertsema, E. M. *Chem. Rev.* **2000**, *100*, 1789–1816.
(14) Szaciłowski, K. *Chem. Rev.* **2008**, *108*, 3481–3548.
(15) Matharu, A. S.; Jeeva, S.; Ramanujam, P. S. *Chem. Soc. Rev.* **2007**, *36*, 1868–1880.
(16) Kawata, S.; Kawata, Y. *Chem. Rev.* **2000**, *100*, 1777–1788.
(17) Berkovic, G.; Krongauz, V.; Weiss, V. *Chem. Rev.* **2000**, *100*, 1741–1754.
(18) Klajn, R. *Chem. Soc. Rev.* **2014**, *43*, 148–184.
(19) Wojtyk, J. T. C.; Buncel, E.; Kazmaier, P. M. *Chem. Commun.* **1998**, *16*, 1703–1704.
(20) Griffiths, J. *Chem. Soc. Rev.* **1972**, *1*, 481–493.
(21) Bandara, H. M. D.; Burdette, S. C. *Chem. Soc. Rev.* **2012**, *41*, 1809–1825.
(22) Irie, M. *Chem. Rev.* **2000**, *100*, 1685–1716.
(23) Tian, H.; Yang, S. *Chem. Soc. Rev.* **2004**, *33*, 85–97.
(24) Eggers, K.; Fyles, T. M.; Montoya-Pelaez, P. J. *J. Org. Chem.* **2001**, *66*, 2966–2977.
(25) Cordes, T.; Weinrich, D.; Kempa, S.; Riesselmann, K.; Herre, S.; Hoppmann, C.; Rück-Braun, K.; Zinth, W. *Chem. Phys. Lett.* **2006**, *428*, 167–173.
(26) Steinle, W.; Rück-Braun, K. *Org. Lett.* **2003**, *5*, 141–144.
(27) Mallory, F. B.; Mallory, C. W. In *Organic Reactions*; John Wiley & Sons, Inc.: Hoboken, NJ, USA, **1984**; pp 1–456.
(28) Cnossen, A.; Kistemaker, J. C. M.; Kojima, T.; Feringa, B. L. *J. Org. Chem.* **2014**, *79*, 927–935.
(29) Bauer, J.; Hou, L.; Kistemaker, J. C. M.; Feringa, B. L. *J. Org. Chem.* **2014**, *79*, 4446–4455.
(30) Fletcher, S. P.; Dumur, F.; Pollard, M. M.; Feringa, B. L. *Science* **2005**, *310*, 80–82.
(31) Koumura, N.; Geertsema, E. M.; van Gelder, M. B.; Meetsma, A.; Feringa, B. L. *J. Am. Chem. Soc.* **2002**, *124*, 5037–5051.
(32) Kistemaker, J. C. M.; Štacko, P.; Roke, D.; Wolters, A. T.; Heideman, G. H.; Chang, M.-C.; van der Meulen, P.; Visser, J.; Otten, E.; Feringa, B. L. *J. Am. Chem. Soc.* **2017**, *139*, 9650–9661.
(33) Lehn, J.-M. *Chem. - A Eur. J.* **2006**, *12*, 5910–5915.
(34) Greb, L.; Lehn, J.-M. *J. Am. Chem. Soc.* **2014**, *136*, 13114–13117.
(35) Greb, L.; Eichhöfer, A.; Lehn, J.-M. *Angew. Chemie Int. Ed.* **2015**, *54*, 14345–14348.
(36) Wolf, C. *Dynamic Stereochemistry of Chiral Compounds*; Royal Society of Chemistry: Cambridge, **2007**.
(37) Erbas-Cakmak, S.; Leigh, D. A.; McTernan, C. T.; Nussbaumer, A. L. *Chem. Rev.* **2015**, *115*, 10081–10206.
(38) Kinbara, K.; Aida, T. *Chem. Rev.* **2005**, *105*, 1377–1400.
(39) Browne, W. R.; Feringa, B. L. *Nat. Nanotechnol.* **2006**, *1*, 25–35.
(40) Erbas-Cakmak, S.; Leigh, D. A.; McTernan, C. T.; Nussbaumer, A. L. *Chem. Rev.* **2015**, *115*, 10081–10206.
(41) Cheng, C.; Stoddart, J. F. *ChemPhysChem* **2016**, *17*, 1780–1793.
(42) Koumura, N.; Zijlstra, R. W.; van Delden, R. A.; Harada, N.; Feringa, B. L. *Nature* **1999**, *401*, 152–155.
(43) Schliwa, M.; Woehlke, G. *Nature* **2003**, *422*, 759–765.
(44) *Molecular Switches*; Feringa, B. L., Browne, W. R., Eds.; Wiley-VCH Verlag GmbH & Co. KGaA: Weinheim, Germany, **2011**.
(45) Kazaryan, A.; Kistemaker, J. C. M.; Schäfer, L. V; Browne, W. R.; Feringa, B. L.; Filatov, M. *J. Phys. Chem. A* **2010**, *114*, 5058–5067.
(46) Lehn, J.-M. *Proc. Natl. Acad. Sci.* **2002**, *99*, 4763–4768.
(47) Göstl, R.; Senf, A.; Hecht, S. *Chem. Soc. Rev.* **2014**, *43*, 1982–1996.
(48) Szymański, W.; Beierle, J. M.; Kistemaker, H. A. V.; Velema, W. A.; Feringa, B. L. *Chem. Rev.* **2013**,

113, 6114–6178.
(49) Dai, Z.; Lee, J.; Zhang, W. *Molecules* **2012**, *17*, 1247–1277.
(50) Bloom, K.; Joglekar, A. *Nature* **2010**, *463*, 446–456.
(51) Berg, J.; Tymoczko, J.; Stryer, L. In *Biochemistry. 5th edition, Section 34.3*; W H Freeman: New York, **2002**.
(52) Lodish, H.; Berk, A.; Zipursky, S. L.; Matsudaira, P.; Baltimore, D.; Darnell, J. In *Molecular Cell Biology. 4th edition, Section 18.3*; W. H. Freeman: New York, **2000**.
(53) Balzani, V.; Credi, A.; Venturi, M. *Molecular Devices and Machines– A Journey into the Nano World*; Wiley-VCH Verlag GmbH & Co. KGaA: Weinheim, FRG, **2003**.
(54) Kassem, S.; van Leeuwen, T.; Lubbe, A. S.; Wilson, M. R.; Feringa, B. L.; Leigh, D. A. *Chem. Soc. Rev.* **2017**, *46*, 2592–2621.
(55) Shirai, Y.; Morin, J.-F.; Sasaki, T.; Guerrero, J. M.; Tour, J. M. *Chem. Soc. Rev.* **2006**, *35*, 1043–1055.
(56) Shirai, Y.; Osgood, A. J.; Zhao, Y.; Kelly, K. F.; Tour, J. M. *Nano Lett.* **2005**, *5*, 2330–2334.
(57) Vives, G.; Kang, J.; Kelly, K. F.; Tour, J. M. *Org. Lett.* **2009**, *11*, 5602–5605.
(58) Villagómez, C. J.; Sasaki, T.; Tour, J. M.; Grill, L. *J. Am. Chem. Soc.* **2010**, *132*, 16848–16854.
(59) Morin, J.-F.; Shirai, Y.; Tour, J. M. *Org. Lett.* **2006**, *8*, 1713–1716.
(60) Saywell, A.; Bakker, A.; Mielke, J.; Kumagai, T.; Wolf, M.; García-López, V.; Chiang, P.-T.; Tour, J. M.; Grill, L. *ACS Nano* **2016**, *10*, 10945–10952.
(61) Kudernac, T.; Ruangsupapichat, N.; Parschau, M.; Maciá, B.; Katsonis, N.; Harutyunyan, S. R.; Ernst, K.-H.; Feringa, B. L. *Nature* **2011**, *479*, 208–211.
(62) Štacko, P. PhD thesis, *Control of Translational and Rotational Movement at Nanoscale*, Groningen, **2017**.
(63) Heideman, H. unpublished results, University of Groningen.
(64) Chen, K.-Y.; Ivashenko, O.; Carroll, G. T.; Robertus, J.; Kistemaker, J. C. M.; London, G.; Browne, W. R.; Rudolf, P.; Feringa, B. L. *J. Am. Chem. Soc.* **2014**, *136*, 3219–3224.
(65) Maeda, N.; Hirose, T.; Yokoyama, S.; Matsuda, K. *J. Phys. Chem. C* **2016**, *120*, 9317–9325.
(66) Ichimura, K. *Science*, **2000**, *288*, 1624–1626.
(67) Feringa, B. L.; van Delden, R. A. *Angew. Chemie Int. Ed.* **1999**, *38*, 3418–3438.
(68) Schulz, G. E.; Schirmer, R. H. *Principles of Protein Structure*; Springer: New York, **1979**.
(69) Saenger, W. *Principles of Nucleic Acid Structure*; Springer: New York, **1984**.
(70) Tu, Y.; Peng, F.; Adawy, A.; Men, Y.; Abdelmohsen, L. K. E. A.; Wilson, D. A. *Chem. Rev.* **2016**, *116*, 2023–2078.
(71) Yan, Q.; Luo, Z.; Cai, K.; Ma, Y.; Zhao, D. *Chem. Soc. Rev.* **2014**, *43*, 4199–4221.
(72) Green, M. M.; Reidy, M. P.; Johnson, R. D.; Darling, G.; O'Leary, D. J.; Willson, G. *J. Am. Chem. Soc.* **1989**, *111*, 6452–6454.
(73) Prins, L. J.; Timmerman, P.; Reinhoudt, D. N. *J. Am. Chem. Soc.* **2001**, *123*, 10153–10163.
(74) Huck, N. P. M.; Jager, W. F.; de Lange, B.; Feringa, B. L. *Science*, **1996**, *273*, 1686–1688.
(75) Palmans, A. R. A.; Meijer, E. W. *Angew. Chemie Int. Ed.* **2007**, *46*, 8948–8968.
(76) Eelkema, R.; Pollard, M. M.; Vicario, J.; Katsonis, N.; Ramon, B. S.; Bastiaansen, C. W. M.; Broer, D. J.; Feringa, B. L. *Nature* **2006**, *440*, 163.
(77) Bosco, A.; Jongejan, M. G. M.; Eelkema, R.; Katsonis, N.; Lacaze, E.; Ferrarini, A.; Feringa, B. L. *J. Am. Chem. Soc.* **2008**, *130*, 14615–14624.
(78) Chen, C.-T.; Chen, C.-H.; Ong, T.-G. *J. Am. Chem. Soc.* **2013**, *135*, 5294–5297.
(79) Delden, R. A. van; Mecca, T.; Rosini, C.; Feringa, B. L. *Chem. Eur. J.* **2004**, *10*, 61–70.
(80) Pieraccini, S.; Gottarelli, G.; Labruto, R.; Masiero, S.; Pandoli, O.; Spada, G. P. *Chem. Eur. J.* **2004**, *10*, 5632–5639.
(81) Mathews, M.; Zola, R. S.; Hurley, S.; Yang, D.-K.; White, T. J.; Bunning, T. J.; Li, Q. *J. Am. Chem. Soc.* **2010**, *132*, 18361–18366.
(82) Nakano, T.; Okamoto, Y. *Chem. Rev.* **2001**, *101*, 4013–4038.
(83) Cornelissen, J. J. L. M.; Rowan, A. E.; Nolte, R. J. M.; Sommerdijk, N. A. J. M. *Chem. Rev.* **2001**, *101*, 4039–4070.
(84) Green, M. M.; Jha, S. K. *Chirality* **1997**, *9*, 424–427.
(85) Teramoto, A. *Prog. Polym. Sci.* **2001**, *26*, 667–720.
(86) Takei, F.; Yanai, K.; Onitsuka, K.; Takahashi, S. *Chem. Eur. J.* **2000**, *6*, 983–993.
(87) Yashima, E.; Maeda, K.; Nishimura, T. *Chem. Eur. J.* **2004**, *10*, 42–51.
(88) Yashima, E.; Maeda, K. *Macromolecules* **2008**, *41*, 3–12.
(89) Pijper, D.; Feringa, B. L. *Soft Matter* **2008**, *4*, 1349–1372.
(90) Bisoyi, H. K.; Li, Q. *Angew. Chemie Int. Ed.* **2016**, *55*, 2994–3010.
(91) Feringa, B. L.; Browne, W. R. In *Molecular Switches*; Wiley-VCH Verlag GmbH & Co. KGaA: Weinheim, Germany, **2011**; pp 101–106.
(92) Maxein, G.; Zentel, R. *Macromolecules* **1995**, *28*, 8438–8440.

(93) Maxein, G.; Mayer, S.; Müller, M.; Zentel, R. *Am. Chem. Soc. Polym. Prepr. Div. Polym. Chem.* **1996**, *37*, 460–461.
(94) Okamoto, Y.; Matsuda, M.; Nakano, T.; Yashima, E. *Polym. J.* **1993**, *25*, 391–396.
(95) Pijper, D.; Feringa, B. L. *Angew. Chemie Int. Ed.* **2007**, *46*, 3693–3696.
(96) Pijper, D.; Jongejan, M. G. M.; Meetsma, A.; Feringa, B. L. *J. Am. Chem. Soc.* **2008**, *130*, 4541–4552.
(97) van Leeuwen, T.; Heideman, G. H.; Zhao, D.; Wezenberg, S. J.; Feringa, B. L. *Chem. Commun.* **2017**, *53*, 6393–6396.
(98) Iamsaard, S.; Aßhoff, S. J.; Matt, B.; Kudernac, T.; Cornelissen, J. J. L. M.; Fletcher, S. P.; Katsonis, N. *Nat. Chem.* **2014**, *6*, 229–235.
(99) Li, Q.; Fuks, G.; Moulin, E.; Maaloum, M.; Rawiso, M.; Kulic, I.; Foy, J. T.; Giuseppone, N. *Nat. Nanotechnol.* **2015**, *10*, 161–165.
(100) Foy, J. T.; Li, Q.; Goujon, A.; Colard-Itté, J.-R.; Fuks, G.; Moulin, E.; Schiffmann, O.; Dattler, D.; Funeriu, D. P.; Giuseppone, N. *Nat. Nanotechnol.* **2017**, *12*, 540–545.
(101) Williams, G. J.; Domann, S.; Nelson, A.; Berry, A. *Proc. Natl. Acad. Sci.* **2003**, *100*, 3143–3148.
(102) Blanco, V.; Leigh, D. A.; Marcos, V. *Chem. Soc. Rev.* **2015**, *44*, 5341–5370.
(103) Vlatković, M.; Collins, B. S. L.; Feringa, B. L. *Chem. Eur. J.* **2016**, *22*, 17080–17111.
(104) Würthner, F.; Rebek, J. *Angew. Chem. Int. Ed.* **1995**, *34*, 446–448.
(105) Cacciapaglia, R.; Di Stefano, S.; Mandolini, L. *J. Am. Chem. Soc.* **2003**, *125*, 2224–2227.
(106) Imahori, T.; Yamaguchi, R.; Kurihara, S. *Chem. Eur. J.* **2012**, *18*, 10802–10807.
(107) Berryman, O. B.; Sather, A. C.; Lledó, A.; Rebek, J. *Angew. Chem. Int. Ed.* **2011**, *50*, 9400–9403.
(108) Ueno, A.; Takahashi, K.; Osa, T. *J. Chem. Soc. Chem. Commun.* **1980**, No. 17, 837–838.
(109) Peters, M. V; Stoll, R. S.; Kühn, A.; Hecht, S. *Angew. Chem. Int. Ed.* **2008**, *47*, 5968–5972.
(110) Osorio-Planes, L.; Rodríguez-Escrich, C.; Pericàs, M. A. *Org. Lett.* **2014**, *16*, 1704–1707.
(111) Balof, S. L.; P'Pool, S. J.; Berger, N. J.; Valente, E. J.; Shiller, A. M.; Schanz, H.-J. *Dalt. Trans.* **2008**, No. 42, 5791.
(112) Blanco, V.; Carlone, A.; Hänni, K. D.; Leigh, D. A.; Lewandowski, B. *Angew. Chem. Int. Ed.* **2012**, *51*, 5166–5169.
(113) Beswick, J.; Blanco, V.; De Bo, G.; Leigh, D. A.; Lewandowska, U.; Lewandowski, B.; Mishiro, K. *Chem. Sci.* **2015**, *6*, 140–143.
(114) Neilson, B. M.; Bielawski, C. W. *J. Am. Chem. Soc.* **2012**, *134*, 12693–126939.
(115) Neilson, B. M.; Bielawski, C. W. *Organometallics* **2013**, *32*, 3121–3128.
(116) Sud, D.; Norsten, T. B.; Branda, N. R. *Angew. Chemie - Int. Ed.* **2005**, *44*, 2019–2021.
(117) Wang, J.; Feringa, B. L. *Science* **2011**, *331*, 1429–1432.
(118) Vlatković, M.; Bernardi, L.; Otten, E.; Feringa, B. L. *Chem. Commun.* **2014**, *50*, 7773–7775.
(119) Zhao, D.; Neubauer, T. M.; Feringa, B. L. *Nat. Commun.* **2015**, *6*, 6652.
(120) Chen, C.-T.; Tsai, C.-C.; Tsou, P.-K.; Huang, G.-T.; Yu, C.-H. *Chem. Sci.* **2017**, *8*, 524–529.
(121) Berg, J. M.; Tymoczko, J. L.; Stryer, L. *Biochemistry*; Freeman, W. H., Ed.; New York, **2002**.
(122) Cram, D. J.; Cram, J. M. *Acc. Chem. Res.* **1978**, *11*, 8–14.
(123) Zhang, X. X.; Bradshaw, J. S.; Izatt, R. M. *Chem. Rev.* **1997**, *97*, 3313–3362.
(124) Islam, M. R.; Mahdi, J. G.; Bowen, I. D. *Drug Saf.* **1997**, *17*, 149–165.
(125) Muraoka, T.; Kinbara, K.; Aida, T. *Nature* **2006**, *440*, 512–515.
(126) Muraoka, T.; Kinbara, K.; Kobayashi, Y.; Aida, T. *J. Am. Chem. Soc.* **2003**, *125*, 5612–5613.
(127) Vlatkovic, M.; Feringa, B. L.; Wezenberg, S. J. *Angew. Chemie - Int. Ed.* **2016**, *55*, 1001–1004.
(128) Lehn, J.-M.; Rigault, A. *Angew. Chemie Int. Ed. English* **1988**, *27*, 1095–1097.
(129) Stadler, A.-M.; Burg, C.; Ramírez, J.; Lehn, J.-M. *Chem. Commun.* **2013**, *49*, 5733.
(130) Zhao, D.; van Leeuwen, T.; Cheng, J.; Feringa, B. L. *Nat. Chem.* **2017**, *9*, 250-256.
(131) Willner, I.; Rubin, S. *Angew. Chemie Int. Ed. English* **1996**, *35*, 367–385.
(132) Beharry, A. A.; Woolley, G. A. *Chem. Soc. Rev.* **2011**, *40*, 4422–4437.
(133) Lubbe, A. S.; Szymanski, W.; Feringa, B. L. *Chem. Soc. Rev.* **2017**, *46*, 1052–1079.
(134) Gorostiza, P.; Isacoff, E. Y. *Science*, **2008**, *322*, 395–399.
(135) Fehrentz, T.; Schönberger, M.; Trauner, D. *Angew. Chemie Int. Ed.* **2011**, *50*, 12156–12182.
(136) Deiters, A. *ChemBioChem* **2009**, *11*, 47–53.
(137) Velema, W. A.; Szymanski, W.; Feringa, B. L. *J. Am. Chem. Soc.* **2014**, *136*, 2178–2191.
(138) Mayer, G.; Heckel, A. *Angew. Chemie Int. Ed.* **2006**, *45*, 4900–4921.
(139) Kamiya, Y.; Asanuma, H. *Acc. Chem. Res.* **2014**, *47*, 1663–1672.
(140) Dohno, C.; Uno, S.; Nakatani, K. *J. Am. Chem. Soc.* **2007**, *129*, 11898–11899.
(141) Feliciano, M.; Vytla, D.; Medeiros, K. A.; Chambers, J. J. *Bioorg. Med. Chem.* **2010**, *18*, 7731–7738.
(142) Blanco-Lomas, M.; Samanta, S.; Campos, P. J.; Woolley, G. A.; Sampedro, D. *J. Am. Chem. Soc.* **2012**, *134*, 6960–6963.
(143) De Poli, M.; Zawodny, W.; Quinonero, O.; Lorch, M.; Webb, S. J.; Clayden, J. *Science*, **2016**, *352*, 575–

580.
(144) Gorostiza, P.; Volgraf, M.; Numano, R.; Szobota, S.; Trauner, D.; Isacoff, E. Y. *Proc. Natl. Acad. Sci.* **2007**, *104*, 10865–10870.
(145) Schierling, B.; Noel, A.-J.; Wende, W.; Hien, L. T.; Volkov, E.; Kubareva, E.; Oretskaya, T.; Kokkinidis, M.; Rompp, A.; Spengler, B.; Pingoud, A. *Proc. Natl. Acad. Sci.* **2010**, *107*, 1361–1366.
(146) Ud-Dean, S. M. M. *Interdiscip. Sci. Comput. Life Sci.* **2011**, *3*, 79–90.
(147) Tian, T.; Song, Y.; Wang, J.; Fu, B.; He, Z.; Xu, X.; Li, A.; Zhou, X.; Wang, S.; Zhou, X. *J. Am. Chem. Soc.* **2016**, *138*, 955–961.
(148) Chandramouli, B.; Di Maio, D.; Mancini, G.; Brancato, G. *Biochim. Biophys. Acta - Biomembr.* **2016**, *1858*, 689–697.
(149) Shimoboji, T.; Ding, Z. L.; Stayton, P. S.; Hoffman, A. S. *Bioconjug. Chem.* **2002**, *13*, 915–919.
(150) Mogaki, R.; Okuro, K.; Aida, T. *J. Am. Chem. Soc.* **2017**, *139*, 10072–10078.
(151) Lv, Z.; Chen, Z.; Shao, K.; Qing, G.; Sun, T. *Polymers*, **2016**, *8*, 310.
(152) Berg, J. M.; Tymoczko, J. L.; Stryer, L. *Biochemistry*, 5th ed.; Freeman, W. H., Ed.; New York, **2002**.
(153) Kumita, J. R.; Smart, O. S.; Woolley, G. A. *Proc. Natl. Acad. Sci.* **2000**, *97*, 3803–3808.
(154) Flint, D. G.; Kumita, J. R.; Smart, O. S.; Woolley, G. A. *Chem. Biol.* **2002**, *9*, 391–397.
(155) Kusebauch, U.; Cadamuro, S. A.; Musiol, H.-J.; Lenz, M. O.; Wachtveitl, J.; Moroder, L.; Renner, C. *Angew. Chemie Int. Ed.* **2006**, *45*, 7015–7018.
(156) Kusebauch, U.; Cadamuro, S. A.; Musiol, H.-J.; Moroder, L.; Renner, C. *Chem. - A Eur. J.* **2007**, *13*, 2966–2973.
(157) Poloni, C.; Stuart, M. C. A.; van der Meulen, P.; Szymanski, W.; Feringa, B. L. *Chem. Sci.* **2015**, *6*, 7311–7318.
(158) Doran, T. M.; Ryan, D. M.; Nilsson, B. L. *Polym. Chem.* **2014**, *5*, 241–248.
(159) Cochran, A. G.; Skelton, N. J.; Starovasnik, M. A. *Proc. Natl. Acad. Sci.* **2001**, *98*, 5578–5583.
(160) Coskun, A.; Banaszak, M.; Astumian, R. D.; Stoddart, J. F.; Grzybowski, B. A. *Chem. Soc. Rev.* **2012**, *41*, 19–30.
(161) Press Release: The Nobel Prize in Chemistry 2016, https://www.nobelprize.org/nobel_prizes/chemistry/laureates/2016/press.html.
(162) Abendroth, J. M.; Bushuyev, O. S.; Weiss, P. S.; Barrett, C. J. *ACS Nano* **2015**, *9*, 7746–7768.
(163) Kay, E. R.; Leigh, D. A. *Angew. Chemie Int. Ed.* **2015**, *54*, 10080–10088.
(164) Peplow, M. *Nature* **2015**, *525*, 18–21.
(165) Astumian, R. D. *Science*, **1997**, *276*, 917–922.
(166) Astumian, R. D. *Phys. Chem. Chem. Phys.* **2007**, *9*, 5067–5083.
(167) Cheng, C.; McGonigal, P. R.; Stoddart, J. F.; Astumian, R. D. *ACS Nano* **2015**, *9*, 8672–8688.
(168) Deng, H.; Olson, M. A.; Stoddart, J. F.; Yaghi, O. M. *Nat. Chem.* **2010**, *2*, 439–443.
(169) Mattia, E.; Otto, S. *Nat. Nanotechnol.* **2015**, *10*, 111–119.
(170) Watch Fire Ants Use Their Bodies To Form Living Architecture | Science | Smithsonian http://www.smithsonianmag.com/science-nature/watch-fire-ants-use-their-bodies-to-form-living-architecture-180947854/.
(171) Nanotechnology in fiction https://en.wikipedia.org/wiki/Nanotechnology_in_fiction.